Appendix B

Periphyton Analysis

The Periphyton Control Model and its Application to the Grande Ronde River, Oregon

State of Oregon
Department of Environmental Quality
April 2000

Contents

Tables

Figures

1 Introduction

Excessive growth of algae and other autotrophs in natural waters can result in significant diel fluctuations in dissolved oxygen and pH which may adversely impact aquatic life. Autotrophs are organisms that obtain energy from sunlight and their materials from non-living sources (Allan, 1995). In streams, autotrophs include periphyton, phytoplankton, and macrophytes. Periphyton include algae and other small autotrophs that are attached to substrate, such as submerged rocks and vegetation. They consist of complex assemblages of diatoms, green algae, and cyanobacteria (blue-green algae) and, to a lessor degree, yellow-brown algae, euglenoids and red algae. Phytoplankton are algae and other small autotrophs which are suspended in the water column. While they can dominate slow moving rivers and backwaters, they generally are not present in significant quantities in fast flowing streams since their reproduction rates are low relative to retention times. Macrophytes include large vascular plants and bryophytes (mosses and liverworts). Some large members of periphyton, such as long filaments of the green alga Cladophora, may also be classified as Macrophytes.

Algae and other autotrophs impact pH and dissolved oxygen levels as they grow and respire. During the day, when algae performs photosynthesis and grows, carbon dioxide is consumed and oxygen produced. At night respiration dominates. Respiration, which occurs at a relatively constant rate both day and night, has the opposite effect of consuming oxygen and producing carbon dioxide. The net result is that during the day photosynthesis dominates and increases water column concentrations of oxygen while decreasing carbon dioxide concentrations. At night respiration dominates, which decreases oxygen concentrations and increases carbon dioxide concentrations.

Carbon dioxide, when introduced into an aqueous solution, combines with water to form carbonic acid (Chapra, 1997),

$$CO_2 + H_2O \leftrightarrow H_2CO_3$$

The carbonic acid, in turn, dissociates into ionic form,

$$H_2CO_3 \leftrightarrow HCO_3^- + H^+$$

This increases the hydrogen ion concentration, and consequently lowers the pH. Therefore, during the day as algae consume carbon dioxide pH increases, while at night as algae produce carbon dioxide pH declines. Through this process algae can cause large diurnal fluctuations in dissolved oxygen and pH which may result in water quality standards violations. Low oxygen levels can suffocate aquatic organisms, while excessively high or low pH levels can cause toxic effects ranging from growth and reproduction limitations to death.

The extent to which benthic carbon dioxide and oxygen fluxes impact water column pH and dissolved oxygen depends not only on the magnitude of the fluxes, but also on the water depth and the reaeration rate. Water depth controls the mass of water influenced by the fluxes. Reaeration controls the rate that carbon dioxide and oxygen is transferred between the water column and atmosphere. Therefore, for a given set of flux rates, pH and dissolved oxygen fluctuations will be greater in shallow streams with poor aeration than in deep streams with good aeration.

2 Periphyton Control Model

2.1 Introduction

A numerical model has been developed to simulate periphyton in streams and evaluate the impact of potential control measures on diurnal pH and dissolved oxygen. The model, referred to as the Periphyton Control Model or PCM, is designed for relatively fast flowing streams in which the algae present is dominated by periphyton. Consequently, all algae present in the system is treated as periphyton. While the model is designed for periphyton, it is calibrated on observed oxygen data and, therefore, also works well for streams in which a significant portion of oxygen production is due to phytoplankton or macrophytes. The following provides an overview of the equations used in PCM.

The change in periphyton concentrations with time is calculated as follows:

$$\frac{dP}{dt} = (G_P - D_P - F_{slough})P \qquad \text{(eq. 1)}$$

where :

P = periphyton concentrat ion, gC/m^2

G_P = algal growth rate, day^{-1}

D_P = algal death or respiratio n rate, day^{-1}

F_{slough} = algal loss due to non - respiratio n related loss mechanisms , day^{-1}

Periphyton is modeled in terms of algal carbon in order to facilitate carbonate system modeling. Output is also provided in terms of chlorophyll, with conversion via literature derived chlorophyll to carbon ratios.

The equation for dissolved oxygen is:

$$\frac{dO_2}{dt} = (G_P - D_P)\frac{P}{H}a_{oc} + K_a(O_{2sat} - O_2) - K_d(BOD) \qquad \text{(eq. 2)}$$

where :

O_2 = dissolved oxygen, g/m^3

H = depth, m

a_{oc} = oxygen to algal carbon ratio, gO_2/gC

K_a = reaeration coefficient, day^{-1}

$O_{2,sat}$ = dissolved oxygen at saturation, g/m^3

K_d = BOD oxidation coefficient, day^{-1}

BOD = biochemical oxygen demand, g/m^3

Photosynthesis and respiration affect water column oxygen and carbon dioxide concentrations as follows (Stumm and Morgan, 1981):

$$106CO_2 + 16NO_3^- + HPO_4^{2-} + 122H_2O + 18H^+ \Leftrightarrow \underbrace{\{C_{106}H_{263}O_{110}N_{16}P_1\}}_{\text{"algae"}} + 138O_2 \quad \text{(eq. 3)}$$

$$106CO_2 + 16NH_4^+ + HPO_4^{2-} + 108H_2O \Leftrightarrow \{C_{106}H_{263}O_{110}N_{16}P_1\} + 107O_2 + 14\text{H}^+ \quad \text{(eq. 4)}$$

The forward reaction is photosynthesis and the reverse respiration. The first equation is for nitrate as the nitrogen source and the second for ammonia. As shown, depending upon the nitrogen source, anywhere from 107 to 138 moles of oxygen can be produced per mole of algae generated. Since each mole of algae contains 106 moles of carbon, this equates to 1.009 to 1.302 moles of oxygen produced per mole of water column carbon consumed.

In order to model periphyton, the growth and respiration rates, sloughing rates, and periphyton mass must be known. Since these are very difficult to accurately measure directly, PCM calculates them based on observed conditions. Growth rates are estimated using observed temperatures and nutrient concentrations, solar insolation either directly measured or from a separate temperature model, and observed channel geometry and stream flow rates. Algal respiration rates, sloughing rates, and mass are then derived via mass balance calculations using observed diurnal dissolved oxygen concentrations.

2.2 Derivation of Algal Growth Rate, G_P

The algal growth rate, G_P, is estimated for each timestep (usually every 15 min to 1 hr) using observed data and literature derived relationships. Algae requires light, nutrients, and heat to grow. If quantities of any of these are insufficient for algal growth needs, algal growth will be limited. This is expressed mathematically as follows:

$$\begin{aligned} Gp &= G_{max} \bullet (\text{temperature effect}) \bullet (\text{light effect}) \bullet (\text{nutrient effect}) \\ &= G_{max} \bullet G(T) \bullet G(I) \bullet G(N) \end{aligned} \quad \text{(eq. 5)}$$

In this equation G_{max} is the maximum growth rate of the algae at 20°C under optimal light and nutrient concentrations and G(T), G(I), and G(N) are factors which adjust the growth rate for other temperature, light and nutrient conditions.

2.3 Nutrient Effect, G(N)

Phosphorus and nitrogen are essential nutrients with potential for limiting periphyton growth. Both are present in natural waters in several forms, not all of which can be directly used by algae. The phosphorus form that is readily available for algal growth is the soluble reactive phosphorus (SRP, which is equivalent to dissolved orthophosphate, measured as P). Other less available forms include inorganic phosphorus attached to soil particles and organic particulate phosphorus. Nitrogen forms that are readily available for growth are the dissolved inorganic nitrogen (DIN) forms ammonia, nitrite and nitrate. Nitrogen in the form of organic nitrogen is not directly available. Note that while particulate phosphorus is not readily available for algal growth, some may become available through diagenesis or desorption and flux from the sediment.

Similarly, organic nitrogen may become available through conversion to ammonia in the water column or the benthic layer.

Control of excessive algal concentrations frequently is focused on reducing algal growth rates by controlling the nutrients nitrogen and phosphorus. At low nutrient concentrations algal growth is inhibited while at high nutrient concentrations algal nutrient demands are fully met and growth is limited only by temperature and available light. The algal growth rate dependence on nutrients is represented by the relationship shown in Figure B-1:

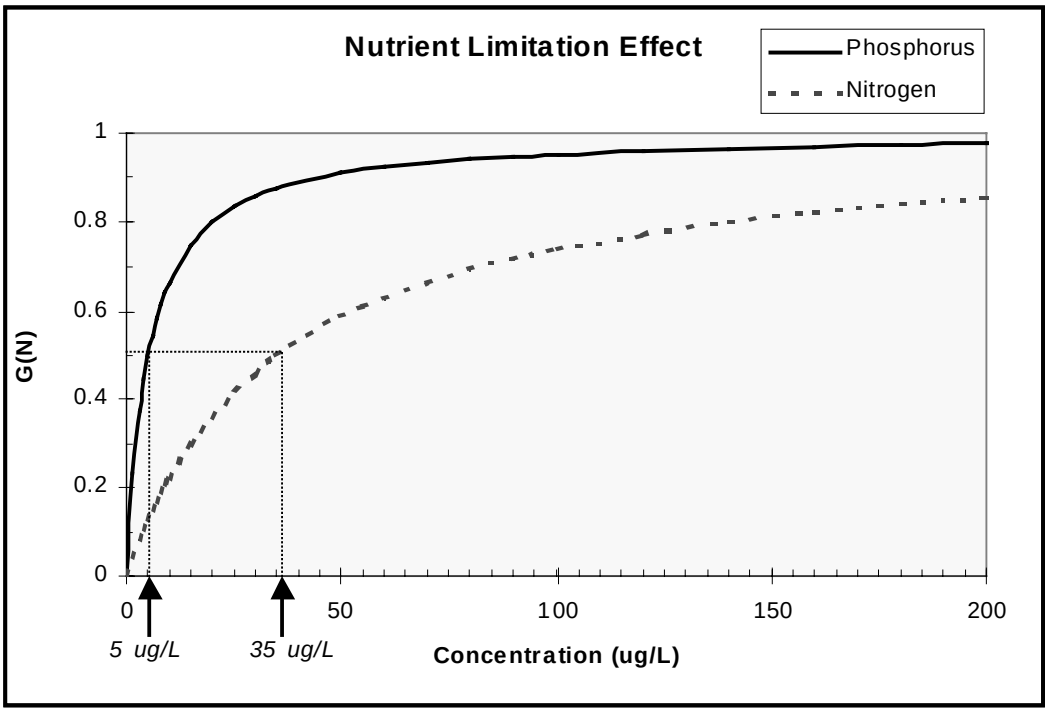

Figure B- 1. Nutrient Limitation Factor, G(N)

As shown, at a nutrient concentration, N, of zero, G(N) is zero and there is no algal growth. As N increases, G(N) increases until it approaches unity, at which point subsequent increases in nutrient concentrations result in insignificant increases in the algal growth rate. At this point the water can be viewed as saturated with the nutrient with respect to algal growth. An equation which represents this relationship is the Michaelis-Menten equation, as follows:

$$G(N) = \frac{N}{K_{mN} + N}$$

where K_{mN} is the nutrient concentration at which G(N) is 0.5 and is referred to as the Michaelis half-saturation constant. For phosphorus, typical half-saturation constants range from 1 to 5 μg P/L for phytoplankton (Thomann and Mueller, 1987) and from 4 to 8 μg P/L for periphyton (USEPA, 1985), although constants significantly outside these ranges have been identified. For illustrative purposes, the Michaelis-Menton equation for a phosphorus half-saturation constant of 5 ug/L is plotted on Figure B-1. Since the stoichiometric ratio of algal cellular nitrogen to phosphorus is about 7 on a mass basis (Section 4.4 below), the corresponding half-saturation constant for nitrogen is 35 ug/L. The Michaelis-Menton equation for nitrogen is also plotted on

Figure B-1. As shown, at concentrations several times greater than the half-saturation constant, G(N) approaches 1 and the nutrient does not significantly limit growth. For example, at a phosphorus concentration of 25 μg/L, which is 5 times the phosphorus half-saturation constant, G(N) is 0.83, indicating a growth rate 83% of the maximum rate. At concentrations less than the half-saturation constants, algal growth is severely inhibited.

Several options are available for combining limitation due to nitrogen with limitation due to phosphorus (USEPA, 1985). These include: 1) a multiplicative formula in which the nutrient limitation factor for phosphorus, G(phosphorus), is multiplied by the limitation factor for nitrogen, G(nitrogen), to obtain G(N); 2) a minimum formulation in which the most severely limiting factor is assumed to limit growth; 3) a harmonic mean formulation which combines the reciprocal of each limiting factor; and 4) an arithmetic formulation which uses the average of each limiting factor.

The second method, which is the approach used in many recent algal models (USEPA 1985), is the method utilized in PCM. In this formulation the nutrient in shortest supply relative to algal needs defines the nutrient limitation factor, G(N). For example, if a water contains 50 μg/L of SRP and 100 μg/L of DIN, G(phosphorus) would be 50/(5+50) = 0.91 and G(nitrogen) would be 100/(35+100) = 0.74. G(N) would therefore be the lesser of the two, i.e., 0.74.

2.3.1 Light Effect, G(I)

Since the energy source for algal growth is light, algae growth responds positively to increased light levels. This is illustrated by Figure B-7 and represented by the following equation (Thomann and Mueller, 1987):

$$G(I) = \frac{I}{I_s}\exp\left(\frac{-I}{I_s}+1\right) \qquad \text{(eq. 6)}$$

where:

I = light intensity at algae depth (Ly)

I_s = saturating light intensity (Ly)

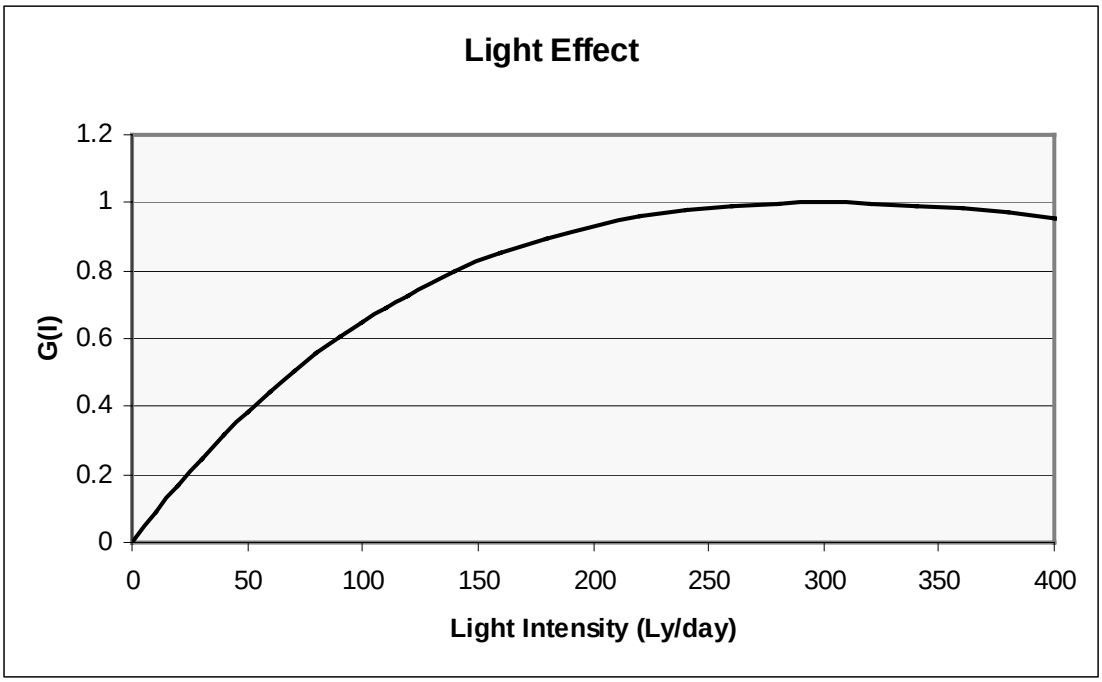

Figure B- 2. Light Limitation Factor G(I)

The light intensity which impacts periphyton is a function of the light intensity at the surface, the light absorption in the water column, and water depth. Light intensity at the surface is a function of location, time of year, time of day, meteorological conditions, and shading from topographic features or riparian vegetation. Light extinction in the water column is a function of water depth and water turbidity due to inorganic solids, detrital particles, suspended phytoplankton, etc.

In order to calculate G(I), data is needed on light intensity. While historical data is available for other parameters affecting algal growth, such as nutrient concentrations, temperature, water depth, etc., historical data is generally not available on light intensity. Light intensity may be derived using a temperature model calibrated on observed temperature, shade and depth data. The estimated solar radiation is converted to photoactive solar radiation by mutiplying it by a factor in the range 0.4 to 0.5.

Light extinction with depth is a calculated via (Thomann and Mueller, 1987):

$$I = I_{surface} \exp(-K_e H) \qquad \text{(eq. 7)}$$

where: I = photoactive active solar radiation at the benthos, Ly/min
$I_{surface}$ = photoactive radiation which penetrates the surface, Ly/min
K_e = light extinction coefficient, 1/m
H = depth, m

K_e is a function of turbidity and ranges from less than 0.5 for relatively clear waters to 2 or more for highly turbid waters (Thomann and Mueller, 1987).

2.3.2 Temperature Effect, G(T)

The temperature factor is calculated as follows (Thomann and Mueller, 1987):

$$G(T) = (1.066)^{T-20} \qquad \text{(eq. 8)}$$

Figure B-6 presents a plot of the equation 6. As shown, as temperature increases, the growth rate increases. Therefore, stream reaches with elevated temperatures have greater growth rates and are more likely to experience pH and dissolved oxygen violations than those with lower temperatures.

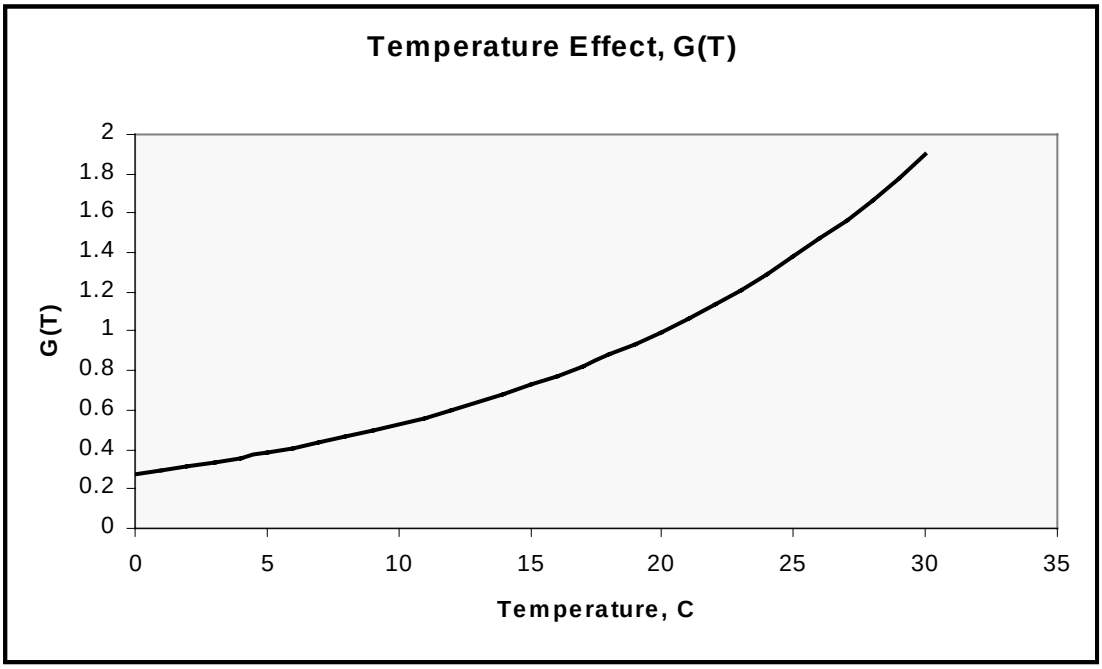

Figure B- 3. Temperature Limitation Factor, G(T)

Note that shade has a compound effect on algal growth rate. Increasing shade directly reduces G(light), and indirectly reduces G(T) by reducing stream temperatures. Therefore, shade can significantly reduce algal activity.

2.4 Mass balance to estimate flux of oxygen due to P-R, reaeration, and BOD oxidation

Now that the algal growth rates, G_P, have been estimated, the oxygen mass balance for each time step can be calculated. Oxygen enters and leaves the water column through algal production and respiration (P-R), atmospheric exchange, and BOD oxidation.

The net oxygen flux at each time step is derived as follows (Brown and Barnwell, 1987):

$$Flux_{O_2Net} = Flux_{O_2P-R} + Flux_{O_2K_a} + Flux_{O_2BOD} \qquad \text{(eq.9)}$$

where:

$Flux_{O_2P-R}$ = net oxgen flux due to algae (production - respiration), $g/m^3 - day$

$Flux_{O_2K_a}$ = oxygen flux due to reaeration, $g/m^3 - day$

$Flux_{O_2BOD}$ = oxygen flux due to BOD oxidation (always negative), $g/m^3 - day$

The net oxygen flux, $Flux_{O_2Net}$, is simply the change in dissolved oxygen from one time step to the next. Usually time steps of 1 hour are used, but shorter time steps may be needed in highly aerated waters.

The oxygen atmospheric flux due to reaeration, $Flux_{O_2K_a}$, is calculated using estimated reaeration rates and the observed oxygen deficit, as follows (Brown and Barnwell, 1987):

$$Flux_{O_2K_a} = K_a(O_{2,sat} - O_2) \qquad \text{(eq.10)}$$

where:

$Flux_{O_2K_a}$ = oxygen flux due to reaeration, $g/m^3 - day$

K_a = reaeration coefficient, day^{-1}

$O_{2,sat}$ = dissolved oxygen at saturation, g/m^3

O_2 = dissolved oxygen, g/m^3

Reaeration coefficients are estimated using empirical formulations from the literature in which reaeration is correlated to velocity and depth or velocity and slope. Three formulations are provided in the model: O'Connor and Dobbins; Owens, Edwards and Gibbs; and Tsivoglou-Wallace (Brown and Barnwell, 1987). The optimum equation to apply to the Grande Ronde was determined to be the Owens, et al., equation, as follows (Owens 1964):

$$K_{a,20} = \frac{21.7u^{0.67}}{H^{1.85}}$$

where:

$K_{a,20}$ = reaeration coefficient at 20^oC

u = velocity, ft/s

H = mean depth, ft

The oxygen flux due to BOD oxidation, $Flux_{O_2BOD}$, is derived using observed BOD concentrations for the reach being modeled and estimated BOD decay rates. In streams with significant oxygen production due to algae the flux due to BOD oxidation is usually quite small relative to the other components of the oxygen balance. It does not impact the diel oxygen fluctuation, but rather lowers the daily average oxygen concentration.

The net oxygen flux due to algae can now be calculated by solving eq. 9 for $Flux_{O_2P-R}$.

2.5 Derivation of Periphyton Respiration Rates, Sloughing Rates, and Mass

Now that the net oxygen flux rate due to algal production and respiration, $Flux_{O_2P-R}$, has been estimated for each time step, the gross algal production rate, $Flux_{O_2P}$, and gross algae respiration rate, $Flux_{O_2R}$, can be derived for each step. The methodology is as follows:

Since no algal production occurs at night, $Flux_{O_2R}$ at night equals $Flux_{O_2P-R}$. The average nighttime respiration flux rate and average nighttime temperature is used to derive a temperature corrected respiration flux rate at 20°C via the following Streeter-Phelps type formulation (Brown and Barnwell, 1987):

$$Flux_{O_2R,20} = Flux_{O_2R} \Big/ \theta^{(T-20)} \quad \text{(eq. 11)}$$

θ is typically around 1.047 and is determined during model calibration (Brown and Barnwell, 1987).

$Flux_{O_2R}$ is subsequently derived for the daytime time steps using this relationship. $Flux_{O_2P}$ is then derived for via $Flux_{O_2P} = Flux_{O_2P-R} - Flux_{O_2R}$.

Now that $Flux_{O_2P}$ is known for each daytime time step, the periphyton mass, P, may be calculated as follows (Thomann and Mueller, 1987):

$$Flux_{O_2P} = G_P P a_{oc} \Delta t$$

$$\text{Therefore} \quad P = \frac{Flux_{O_2P}}{(G_P)(a_{oc})(\Delta t)} \quad \text{(eq.12)}$$

where

P = periphyton mass, gC/m^3

Δt = timestep, days

The respiration rate, D_P, is derived for each daytime time step via

$$D_P = G_P - \frac{Flux_{O_2P-R}}{(G_P)(a_{oc})(\Delta t)} \quad \text{(eq. 13)}$$

The respiration rate at 20°C, D_{P20}, is then derived using the average daytime temperature and the 24 hour average D_P is derived using the 24 hour average temperature.

Finally, the daily average periphyton mass is calculated as follows:

$$P_{average} = \frac{\sum Flux_{O_2P_{t=1-24}}}{(a_{oc})(G_{P,avg})} \qquad \text{(eq.14)}$$

where:

$\sum Flux_{O_2P_{t=1-24}}$ = total gross oxygen production by algae for 24 hrs

$G_{P,avg}$ = daily average algal growth rate

P is converted to an areal basis, gC/m^2, by multiplying by the depth.

F_{slough} is derived by assuming that the periphyton mass has reached it's maximum extent during the critical model calibration condition (usually late July through mid August) and is in a state of dynamic equilibrium (i.e., the mass at the end of the day equals the mass at the beginning). Therefore:

$$F_{slough} = G_{P,avg} - D_{P,avg} \qquad \text{(eq. 15)}$$

2.6 Ammonia preference factor

As discussed above in Section 2.1 (equations 3 and 4), depending upon the nitrogen source, from 107 to 138 moles of oxygen are produced for every 106 moles of carbon converted to algae. In mass terms, this equates to 2.67 to 3.47 g O_2 produced per g algal carbon generated. While both ammonia and nitrate are available for uptake by algae, for physiological reasons the preferred form is ammonia. This preference for ammonia is quantified via the ammonia preference factor, β_{NH4}, as follows (Thomann and Fitzpatrick, 1982; Ambrose et. al, 1988):

$$\beta_{NH4} = NH_4N\left(\frac{NO_3N}{(K_{mN} + NH_4N)(K_{mN} + NO_3N)} + \frac{K_{mN}}{(NH_4N + NO_3N)(K_{mN} + NO_3N)}\right) \qquad \text{(eq.16)}$$

where:

NH_4N = ammonia nitrogen concentration, $^{mg}/_{L}$

NO_3N = nitrate nitrogen concentration, $^{mg}/_{L}$

K_{mN} = michaelis-menton half saturation concentration for nitrogen, $^{mg}/_{L}$

The mass of dissolved oxygen produced per mass of water column CO_2 converted to algal carbon is calculated by PCM as follows (Stumm and Morgan, 1981):

$$a_{oc,NH_4,mol} = 107 \text{ moles } O_2 / 106 \text{ moles C} = 1.0094 \quad {}^{molesO_2}\!/_{molesC}$$

$$a_{oc,NO_3,mol} = 138 \text{ moles } O_2 / 106 \text{ moles C} = 1.3019 \quad {}^{molesO_2}\!/_{molesC}$$

$$a_{co,NH_4} = {}^{1}\!/_{a_{oc,NH_4,mol}} \bullet \left({}^{12}\!/_{32}\right) \quad {}^{gC}\!/_{gO_2}$$

$$a_{co,NO_3} = {}^{1}\!/_{a_{oc,NO_3,mol}} \bullet \left({}^{12}\!/_{32}\right) \quad {}^{gC}\!/_{gO_2}$$

$$a_{co} = \beta_{NH4} a_{co,NH_4} + (1 - \beta_{NH4}) a_{co,NO_3} \quad {}^{gC}\!/_{gO_2}$$

$$a_{oc} = {}^{1}\!/_{a_{co}} \quad {}^{gO_2}\!/_{gC}$$

where :

$a_{oc,NH_4,mol}$ = moles O_2 produced per mole CO_2 converted to algal C if ammonia is N source

$a_{oc,NO_3,mol}$ = moles O_2 produced per mole CO_2 converted to algal C if nitrate is N source

a_{co} = mass algal C generated per mass O_2 produced

a_{oc} = mass O_2 produced per mass CO_2 converted to algal C

2.7. Carbonate System

pH is the negative log of the hydrogen ion concentration ($pH = -\log_{10}[H+]$), where [H+] is the hydrogen ion concentration in moles/liter (M). Therefore, waters high in $[H^+]$ are acidic and have a low pH. Modeling the carbonate system to derive pH differs from dissolved oxygen modeling only in the greater complexity of the chemistry. A representation of the inorganic carbon system is presented in Figure B-4 (Chapra, 1997).

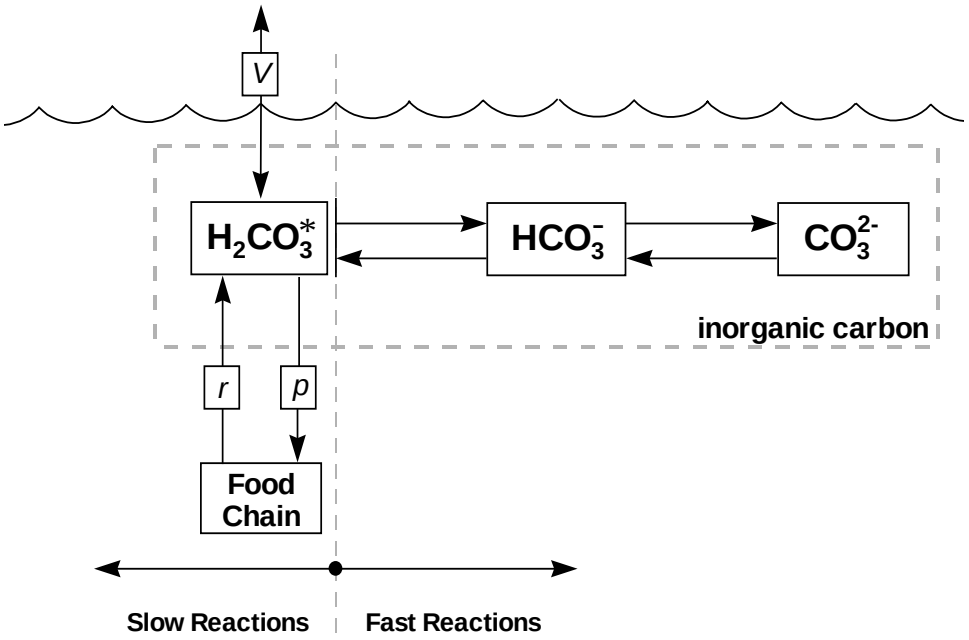

Figure B- 4. Carbonate system

2.7.1. Carbonate system – "Fast" reactions (chemical equilibria)

The dissolved chemical species which make up the carbonate system are aqueous carbon dioxide, $CO_2(aq)$; carbonic acid, H_2CO_3; bicarbonate, HCO_3^-; and carbonate, $CO_3^=$; as follows (Snoeyink and Jenkins, 1980):

$$CO_2(aq) + H_2O \Leftrightarrow H_2CO_3$$
$$H_2CO_3 \Leftrightarrow H^+ + HCO_3^-$$
$$HCO_3^- \Leftrightarrow H^+ + CO_3^{2-}$$

Therefore, as CO_2 is added to a water, the hydrogen ion concentration is increased and the pH decreased. Because it is difficult to distinguish between $CO_2(aq)$ and H_2CO_3 and because the proportion present as H_2CO_3 is negligible, a combined species, $H_2CO_3^*$, is used to represent $CO_2(aq)$ plus H_2CO_3, as follows (Chapra, 1997):

$$CO_3^{2-} \Leftrightarrow HCO_3^- \Leftrightarrow H_2CO_3^* \Leftrightarrow CO_2(g)$$

where $CO_2(g)$ is gaseous carbon dioxide.

As shown by Figure B-4, carbon dioxide is consumed by algae during photosynthesis, generated during respiration, and fluxes between the water column and the atmosphere in a direction that is dependent upon the carbon dioxide deficit. The biologically induced fluxes of CO_2 between algae and the water column and the physically induced fluxes between the water column and the atmosphere are termed "slow" reactions because they occur slowly compared to the "fast" chemical equilibrium reactions which distribute inorganic carbon between carbon dioxide, carbonic acid, bicarbonate, and carbonate.

Equilibrium constants for the inorganic carbon system are as follows (Stumm & Morgan, 1981):

$$K_1 = \frac{[H^+][HCO_3^-]}{[H_2CO_3^*]} \approx 10^{-6.3} \quad \text{(eq.17)}$$

$$K_2 = \frac{[H^+][CO_3^{2-}]}{[HCO_3^-]} \approx 10^{-10.3} \quad \text{(eq.18)}$$

The exact values for K_1 and K_2 can be computed as follows (Chapra, 1997):

$$pK_1 = \frac{3404.71}{T_a} + 0.032786T_a - 14.8435 \quad \text{(eq.19)}$$

$$pK_2 = \frac{2902.39}{T_a} + 0.02379T_a - 6.498 \quad \text{(eq.20)}$$

$$\text{where: } T_a = \text{absolute temperature, } {}^{o}K$$

Also of importance is the ionization product of water, K_w (Chapra, 1997):

$$K_w = [H^+][OH^-] \approx 10^{-14} \quad \text{(eq.21)}$$

$$pK_w = \frac{4787.3}{T_a} + 7.1321\log_{10} T_a + 0.010365T_a - 22.80 \quad \text{(eq.22)}$$

The inorganic carbon system delineated above consists of five unknowns: $[H_2CO_3^*]$, $[HCO_3^-]$, $[CO_2^=]$, $[H^+]$, and $[OH^-]$ (Chapra, 1997). Therefore, five independent equations are needed to solve for the unknowns. Three of the five are provided by the equilibrium relationships for K_1, K_2, and K_w (equations 17,18, and 21). A fourth is provided by the following equation for total inorganic carbon, TIC (Chapra, 1997):

$$TIC = [H_2CO_3^*] + [HCO_3^-] + [CO_3^{2-}] \quad \text{(eq.23)}$$

$$\text{(units: moles/L = M)}$$

A fifth equation is provided by alkalinity, Alk (Chapra, 1997):

$$Alk = [HCO_3^-] + 2[CO_3^{2-}] + [OH^-] - [H^+] \quad \text{(eq.24)}$$

$$\text{(units: eq/L)}$$

Note that alkalinity is frequently reported as mg/L as $CaCO_3$. Dividing mg/L as $CaCO_3$ by 50 converts to milliequivalents per liter (meq/L) and by 50,000 converts to equivalents per liter (eq/L).

The five equations can be combined to provide the following equation (Cole and Buchak, 1994):

$$Alk = \frac{TIC[H^+]K_1}{[H^+]K_1 + K_1K_2 + [H^+]^2}\frac{[H^+] + 2K_2}{[H^+]} + \frac{K_w}{[H^+]} - [H^+] \quad \text{(eq.25)}$$

Therefore, when alkalinity, total inorganic carbon concentration, and temperature are known, Eq. 25 can be numerically solved to determine the pH.

If the total inorganic concentration is unknown, but alkalinity, temperature and pH are known, TIC can be derived using the following relationships for $\alpha_0, \alpha_1,$ and α_2, which are the fractions of TIC in carbonic acid, bicarbonate, and carbonate, respectively (Chapra, 1997):

$$\alpha_0 = \frac{[H^+]^2}{[H^+]^2 + K_1[H^+] + K_1K_2} \quad \text{(eq.26)}$$

$$\alpha_1 = \frac{K_1[H^+]}{[H^+]^2 + K_1[H^+] + K_1K_2} \quad \text{(eq. 27)}$$

$$\alpha_2 = \frac{K_1K_2}{[H^+]^2 + K_1[H^+] + K_1K_2} \quad \text{(eq. 28)}$$

and

$$[H_2CO_3^*] = \alpha_o TIC \quad \text{(eq. 29)}$$

$$[HCO_3^-] = \alpha_1 TIC \quad \text{(eq. 30)}$$

$$[CO_3^{2-}] = \alpha_2 TIC \quad \text{(eq. 31)}$$

Equations 29 and 31, along with equation 21, can be substituted into eq. 24 to give (Chapra, 1997):

$$0 = \alpha_1 TIC + 2\alpha_2 TIC + \frac{K_w}{[H^+]} - [H^+] - Alk \quad \text{(eq. 32)}$$

which can be readily solved for TIC. $[H_2CO_3^*]$ can then calculated from equation 29.

2.7.2. Carbonate system – "Slow" Reactions (production, respiration and atmospheric exchange)

The pH of a water is a function of the water's total inorganic carbon concentration (TIC), alkalinity (Alk), and the temperature. The addition or removal of carbon dioxide due to algal activity, atmospheric exchange, and BOD oxidation affects the TIC concentration. Therefore, in order to estimate the change in pH due to algal activity, atmospheric exchange, and BOD oxidation, the model calculates the change in TIC due to CO_2 addition or removal and then uses equation 25 to solve for pH.

As discussed in Section 2.1, photosynthesis and respiration affect water column oxygen and carbon dioxide concentrations as follows:

$$106CO_2 + 16NO_3^- + HPO_4^{2-} + 122H_2O + 18H^+ \Leftrightarrow \{C_{106}H_{263}O_{110}N_{16}P_1\} + 138O_2$$

"algae"

$$106CO_2 + 16NH_4^+ + HPO_4^{2-} + 108H_2O \Leftrightarrow \{C_{106}H_{263}O_{110}N_{16}P_1\} + 107O_2 + 14\mathrm{H}^+$$

As shown, for each mole of algae produced during photosynthesis, 106 moles of CO_2 are removed from the water column. During respiration, the reverse occurs. These changes in CO_2 concentrations affect the CO_2 deficit and the net direction and rate of atmospheric exchange.

The direction of atmospheric exchange is determined by the CO_2 deficit. If the CO_2 concentration is less than the saturation concentration, then the deficit is positive and CO_2 fluxes from the atmosphere to the water column. If the deficit is negative, CO_2 leaves the water column. The magnitude of the flux is dependent on the reaeration rate. In highly aerated waters, such as shallow, fast flowing waters with many riffles, the rate of flux is much higher than in deep, sluggish waters.

Carbon dioxide is modeled as follows:

$$\frac{dH_2CO_3^*}{dt} = (D_P - G_P)Pa_{wcCa\lg C} + K_{ac}(H_2CO_3^{*}{}_{sat} - H_2CO_3^*) + \frac{K_d(BOD)}{(32)(1000)} \quad \text{(eq. 33)}$$

where:

$H_2CO_3^*$ = carbon dioxide (plus carbonic acid) concentration, $moles/L$

P = periphyton concentration, volume basis, g/m^3

$a_{wcCa\lg C}$ = moles water column carbon per mole algal carbon (usually 1:1)

K_{ac} = carbon dioxide reaeration coefficient, day^{-1}

$H_2CO_3^{*}{}_{sat} = H_2CO_3^*$ concentration at saturation, $moles/L$

K_d = BOD oxidation coefficient, day^{-1}

BOD = biochemical oxygen demand, g/m^3

32 is conversion from mass to moles

1000 is conversion from m^3 to L

Via equation 33 the TIC concentration and corresponding pH are calculated for each time step.

The CO_2 reaeration coefficient, K_{ac}, is a function of the oxygen reaeration rate, K_a, as follows:

$$K_{ac} = cK_a \quad \text{(eq. 34)}$$

An initial estimate of c of 0.92 is estimated via (Chapra, 1997):

$$c = \left(\frac{32}{M}\right)^{0.25} \quad \text{(eq. 35)}$$

where:

M = molecular weight of CO_2 = 44

The coefficient may subsequently be refined during the calibration process.

Photosynthesis and respiration can also affect the alkalinity, as shown by equations 3 and 4. When nitrate is the nitrogen source, alkalinity is increased during photosynthesis because of the consumption of H^+ (see equation 24). When ammonia is the nitrogen source alkalinity is reduced due to the production of H^+. Therefore, PCM increases the alkalinity by 18 equivalents per mole of nitrate consumed during photosynthesis and decreases the alkalinity by 14 equivalents per mole of ammonia consumed. The opposite occurs when respiration dominates.

As for oxygen, the algal preference factor, β_{NH4}, determines the change in alkalinity for a given change in periphyton. The equivalents of alkalinity produced per mole of algal carbon produced are calculated as follows:

$$a_{alkc} = a_{alkc,NH_4}\beta_{NH4} + a_{alkc,NO_3}(1-\beta_{NH4}) \qquad \text{(eq. 36)}$$

where:

$$a_{alkc,NH_4} = -14 \ {}^{eq}/_{L}$$

$$a_{alkc,NO_3} = +18 \ {}^{eq}/_{L}$$

3 Beneficial Uses, Water Quality Standards and the 303(d) List

3.1 Beneficial Uses

Oregon Administrative Rules (OAR Chapter 340, Division 41, Table 13) lists the designated beneficial uses for which water is to be protected in the Upper Grande Ronde watershed. All reaches in the Upper Grande Ronde watershed are designated for anadromous fish passage, salmonid fish spawning, salmonid fish rearing, and resident fish and aquatic life; as well as other uses including domestic water supply, water contact recreation, irrigation, livestock watering, and fishing.

During the fall, winter and spring period from October 1 through June 30, spawning and egg incubation are beneficial uses in all reaches. More stringent standards apply during these periods for dissolved oxygen and temperature, although the pH standard remains the same.

3.2 303(d) List

The State of Oregon 303(d) list of waterbodies which fail to meet water quality standards for the Grande Ronde is summarized in Table B-1

Table B-1. Grande Ronde River - 303(d) List Summary

Boundaries	Upper MP*	Lower MP*	Parameter
Headwaters to Tanner Gulch		202.0	Sedimentation, Habitat Modification
Tanner Gulch to Clear Ck	202.0	200.5	Sedimentation, Habitat Modification, pH
Clear Ck to Five Points Ck	200.5	165.5	Sedimentation, Habitat Modification, pH, Temperature
Five Points Creek** to Wallowa River	165.5	82.0	Sedimentation, Habitat Modification, pH, Temperature, Dissolved Oxygen, Nutrients, Bacteria, Aquatic Weeds or Algae, Flow Modification

* Mile points from Grande Ronde Drainage Basin map, State of Oregon Water Resources Dept., 1975

**This section effectively reduced in length 33 miles by the State Ditch, which diverts water from MP 150 to MP 117

As shown, all reaches of the Grande Ronde River below MP 202, including the State Ditch, experience standards violations related to excessive periphyton activity. Below MP 165.5, pH, dissolved oxygen, nutrients, and aquatic weeds or algae standards violations occur, indicating that periphyton activity is more severe than above MP 165.5, where only pH violations occur.

3.3 Applicable pH and Dissolved Oxygen Standards

The section of the river modeled (milepoint 151.3 to 184.5) experiences standards violations related to periphyton activity. The entire section modeled experiences pH values which exceed the acceptable range of 6.5 to 9.0, while the lower 14 miles modeled also experience low dissolved oxygen concentrations in violation of the dissolved oxygen standard.

The standards described in Oregon Administrative Rules for dissolved oxygen are somewhat complicated. The applicable dissolved oxygen standard depends on whether the most sensitive species present are cold water (salmonid) or cool water (non-salmonid) species and on whether salmonid spawning and egg incubation occurs. Therefore, applicable dissolved oxygen standards can be both temporally and spatially variable.

For reaches and time periods identified as providing for salmonid spawning and egg incubation, the applicable water column standard is 95% of saturation. For a 3000 ft. elevation, which is roughly the average elevation of the reaches modeled, 95% saturation at 10^{o}C (bull trout temperature criteria) is 9.7 mg/L and at 12.8^{o}C (salmonid spawning temperature criteria) is 9.1 mg/L.

For reaches and time periods identified as providing for cold water aquatic life, including salmonids (other than during spawning and egg incubation), two sets of standards are specified:
1) The lesser of 8.0 mg/L or 90% of saturation as an absolute minimum,
2) 8.0 mg/L as a 30-day average, 6.5 mg/L as a 7-day average of the daily minimums, and 6.0 mg/L as an absolute minimum.

The first standard applies when only limited data is available. The second applies when substantial continuous monitoring data is available, such as is available for the upper Grande Ronde River.

For cool water, non-salmonid species, the standards are:
1) 6.5 mg/L as an absolute minimum
2) 6.5 mg/L as a 30-day average, 5.0 mg/L as a 7-day average of the daily minimums, and 4.0 mg/L as an absolute minimum.

As with cold water species, the second standard applies when substantial continuous monitoring data is available.

Waterbodies identified as providing for cold-water aquatic life are bodies within which salmon, trout, cold-water invertebrates, and other native cold-water species exist throughout all or most of the year (OAR 340-41-455 Table 21) and within which juvenile anadromous salmonids may rear throughout the year. All reaches in the upper Grande Ronde Basin have been identified as providing for cold-water aquatic life.

For pH, the OAR specify that the pH (-log[H^{+}]) shall not fall outside of the range 6.5 to 9.0. When greater than 25% of ambient measurements taken between June and September are greater than pH 8.7, and as resources are available according to priorities set by the Department, the Department shall determine whether the values higher than 8.7 are anthropogenic or natural in origin.

4 Model Calibration – Grande Ronde River

A calibration of the periphyton control model PCM was developed for 33 miles of the Grande Ronde from milepoint 151.3 to 184.5.

4.1 Reaches modeled

The 33 miles of river model were divided into six reaches. These included five of eight mainstem Grande Ronde reaches modeled by ODEQ for temperature using the model Heat Source (Reaches 4 though 8 on Figure B-5), plus one additional downstream reach, Reach 9, which extends from Reach 8 to the State Ditch.

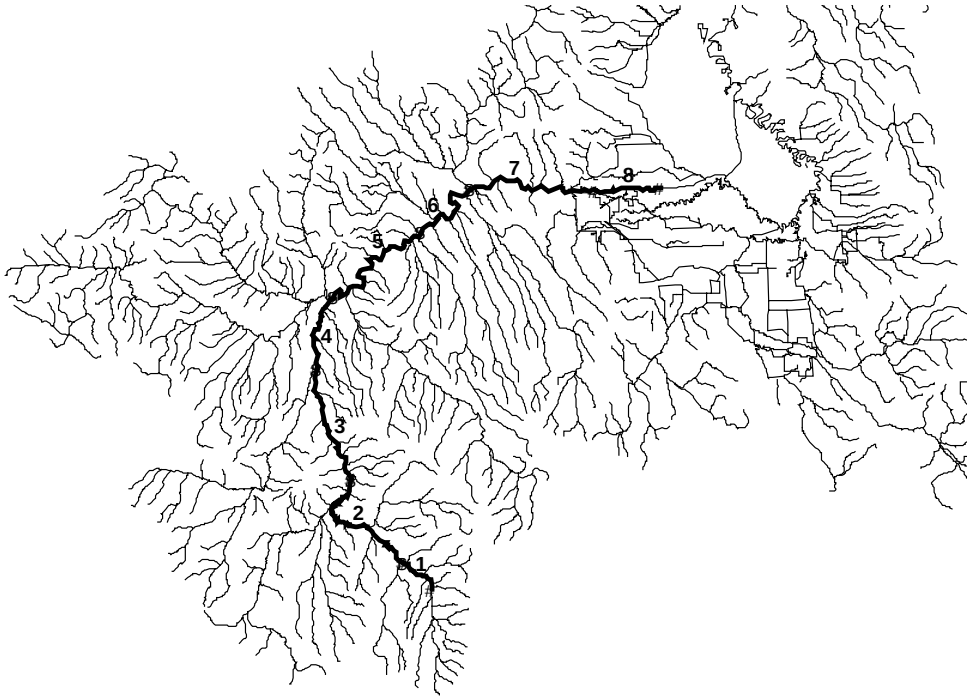

Figure B- 5. Model Reaches

The reaches are described in Table B-2.

Table B- 2. Model Reaches

Reach	Upper Mile Point	Lower Mile Point	Upper Extent	Lower Extent
4	184.5	179.7	Upstream of Fly Ck	Downstream of Meadow Ck
5	179.7	171.0	Downstream of Meadow Ck	Downstream of Jordan Ck
6	171.0	165.5	Downstream of Jordan Ck	Upstream of Five Points Ck
7	165.5	157.3	Upstream of Five Points Ck	Spruce Street (La Grande)
8	157.3	153.8	Spruce Street (La Grande)	Pierce Road
9	153.8	151.3	Pierce Road	Peach Lane

These were selected for PCM calibration because they experience periphyton related standards violations and because diurnal dissolved oxygen and pH data is available for each from paired recording datasondes (Hydrolabs).

4.2 Observed pH and dissolved oxygen

Calibration was performed using Hydrolab data collected by ODEQ in August, 1992. During the survey, a pair of Hydrolabs spaced one mile apart were installed near the downstream end of each of the six reaches. The observed pH, dissolved oxygen, dissolved oxygen saturation and temperature data is presented in Figures B-6 and B-7. An indication of the frequency of dissolved oxygen and pH violations is provided by the box and whisker plots presented in Figures B-8 and B-9 (see Appendix for an explanation of box and whisker plots).

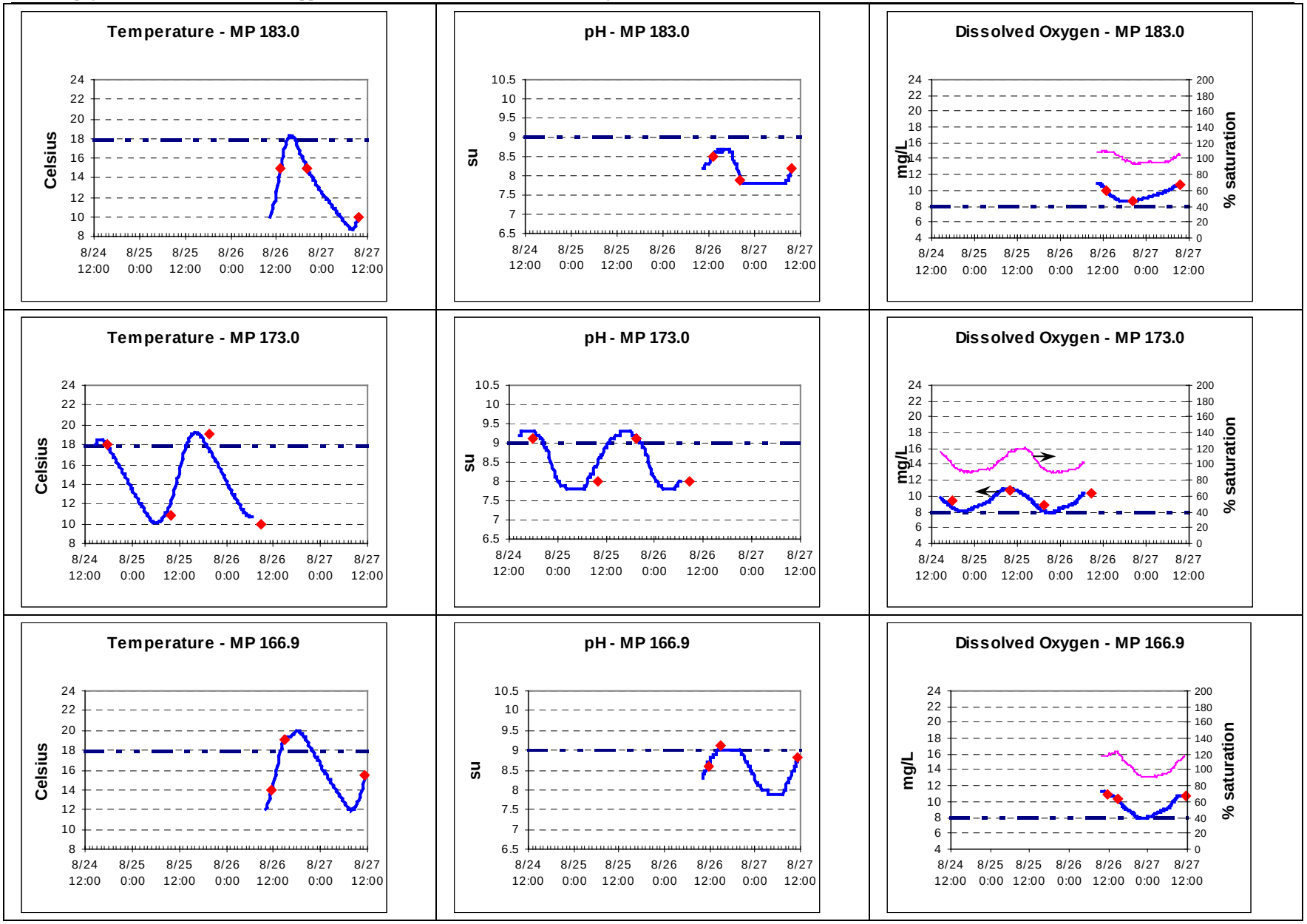

Figure B- 6. Observed continuous monitoring data - August 1992

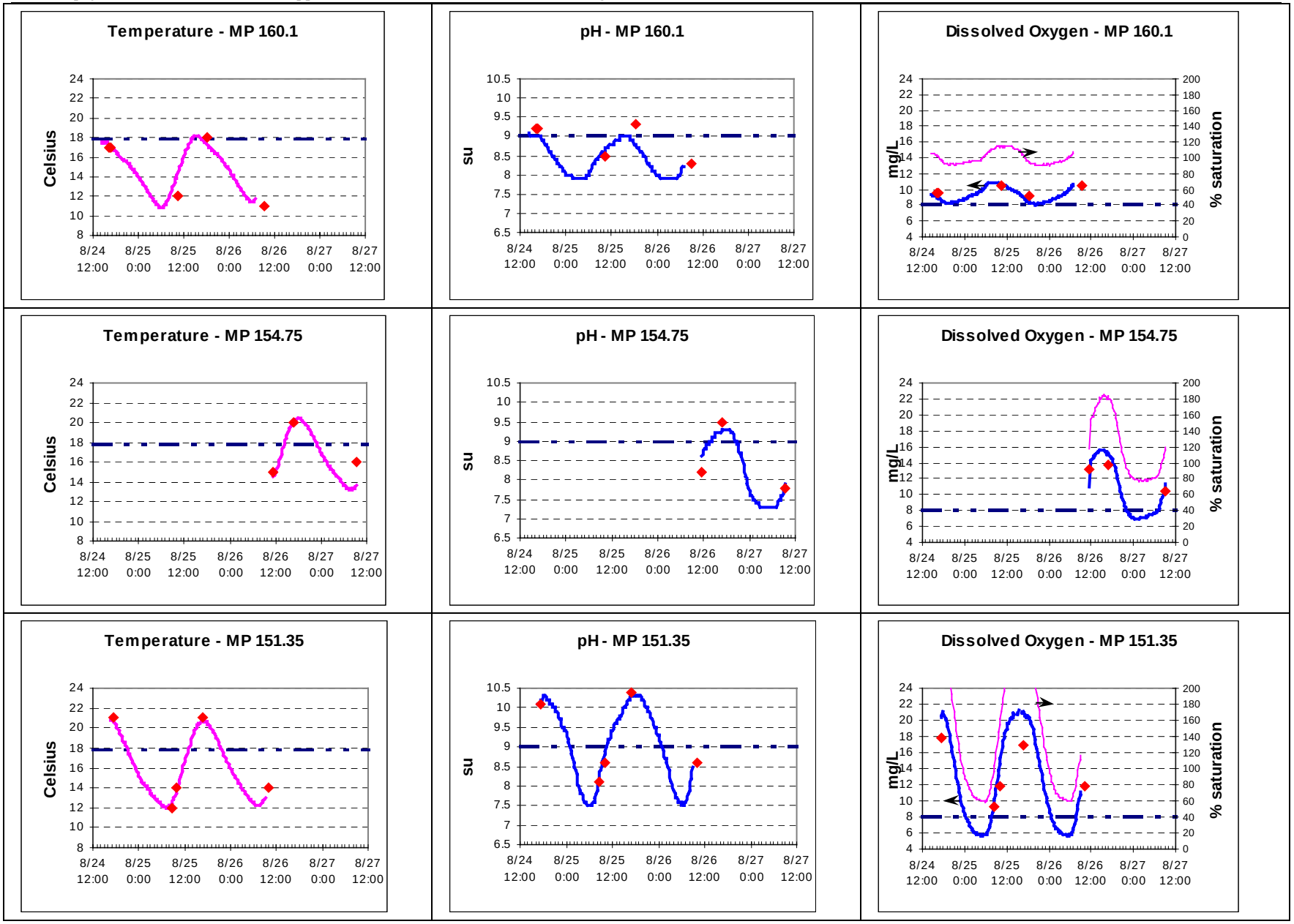

Figure B- 7. Observed continuous monitoring data - August 1992

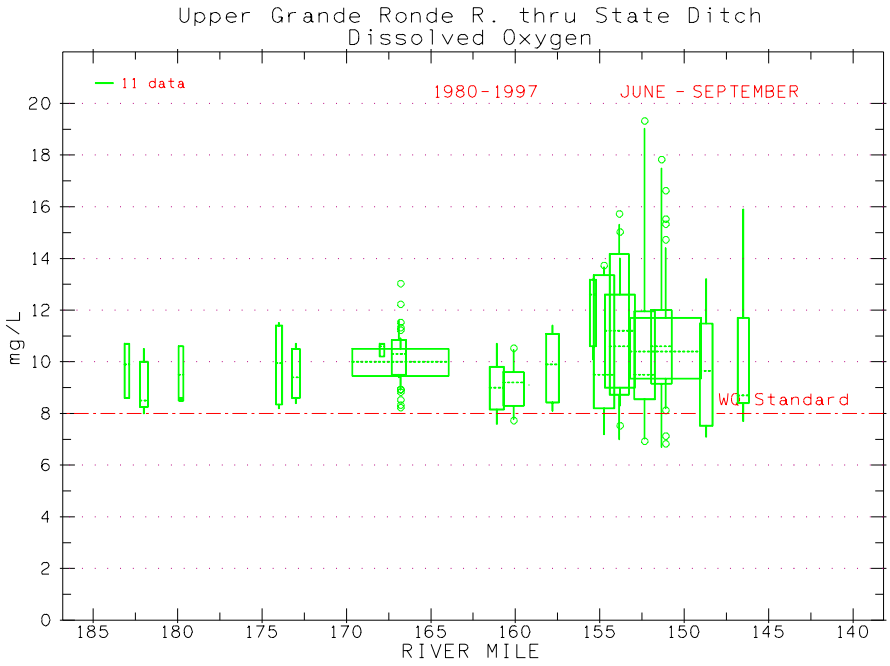

Figure B- 8. Grande Ronde River - Dissolved Oxygen

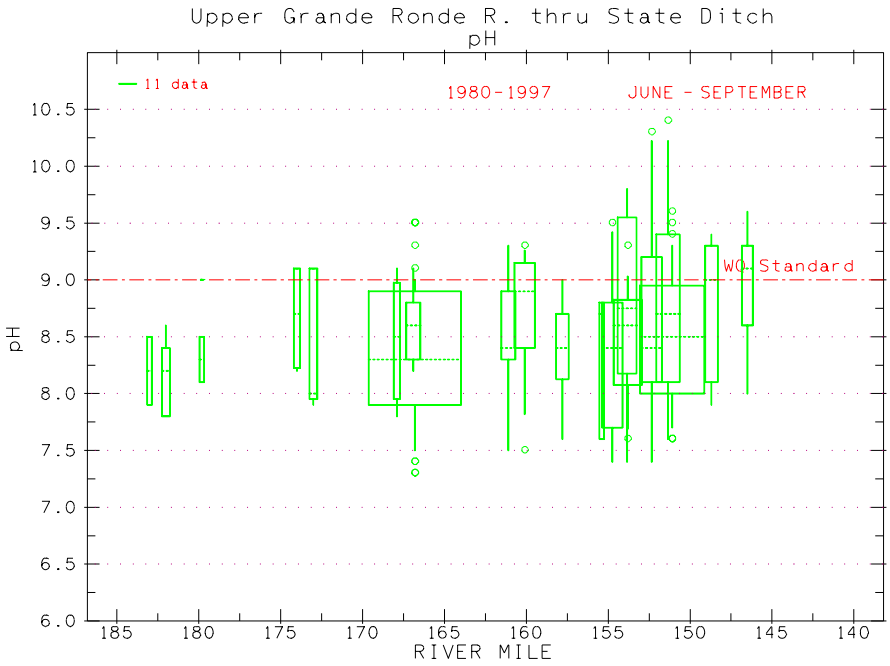

Figure B- 9. Grande Ronde River - pH

Figures B-8 and B-9 present data from ODEQ grabs samples collected during the summer (June-September) from 1980 through 1997. As shown, dissolved oxygen standard violations occurred occasionally below MP 162. pH standard violations were observed more frequently, with occasional violations observed as far upstream as MP 175 and frequent violations observed below MP 155. Note that all observations are from individual grab samples. Since grab samples are usually collected during the day, a daytime bias is possible. This may partially explain the relatively high frequency of pH violations versus dissolved oxygen violations, since in algae dominated systems maximum dissolved oxygen concentrations and pHs generally occur during the day.

The City of LaGrande waste water treatment plant (WWTP) discharge enters the Grande Ronde River at mile point 153.8 (Pierce Lane). Nutrients from the WWTP have been identified as causitive agents for increased algal growth which contributes to the excessive diurnal dissolved oxygen and pH fluctuations (ODEQ, 1995a). Downstream of LaGrande, large DO and pH ranges are observed, indicating the influence of the WWTP. Note, however, that excessive fluctuations also occur upstream of the WWTP point source (the Pierce Lane ambient monitoring station at mile point 153.81 is located upstream of the WWTP discharge and does not appear to be influenced by the discharge). Therefore, nonpoint nutrient sources and other factors also appear to be contributing to the excessive algal growth.

4.3 Reach Geometry

Factors which affect the rate of algal growth and the diurnal dissolved oxygen and pH fluctuations include nutrient concentrations, shade, temperature, stream depth, slope, and velocity,. Reach average velocity, depth and effective shade for each reach came out of the temperature model calibrations developed by ODEQ for August 1992 using the model Heat Source, as described in the draft temperature TMDL document (ODEQ, 1999). For the Heat Source calibration, channel depth and velocity were not directly measured. Instead, detailed data was entered for other inputs, including flow, reach average shade conditions, and wetted widths. Reach average velocities and depths were estimated by adjusting the velocity input to the model until model calculated temperatures matched observed diurnal temperatures.

Inputs to PCM that are provided by Heat Source are presented in Table B-3.

Table B- 3. Inputs to PCM from Heat Source

Reach	Reach Milepoints	Flow m^3/s	Depth m	Velocity m/s	Elevation m	Effective Shade	Slope m/m
4	185.9-182.0	0.479	0.160	0.255	1048	17.5%	0.010125
5	176.4-173.0	0.743	0.221	0.205	960	7.6%	0.003686
6	170.2-166.9	0.798	0.221	0.208	923	6.5%	0.003522
7	163.2-160.1	0.809	0.220	0.220	879	9.9%	0.003614
8	156.7-153.9	0.533	0.246	0.148	833	0.1%	0.003950
9	154.2-151.3	0.473	0.281	0.110	824	0.0%	0.001506

4.4 Nutrients

Summertime (June-September) nutrient data collected by ODEQ for the period 1980 through 1997 for the Grande Ronde is presented below. Figures B-10 and B-11 present total phosphorus and nitrogen data. As shown, nutrient concentrations increase significantly in the Grande Ronde valley below mile point 155.

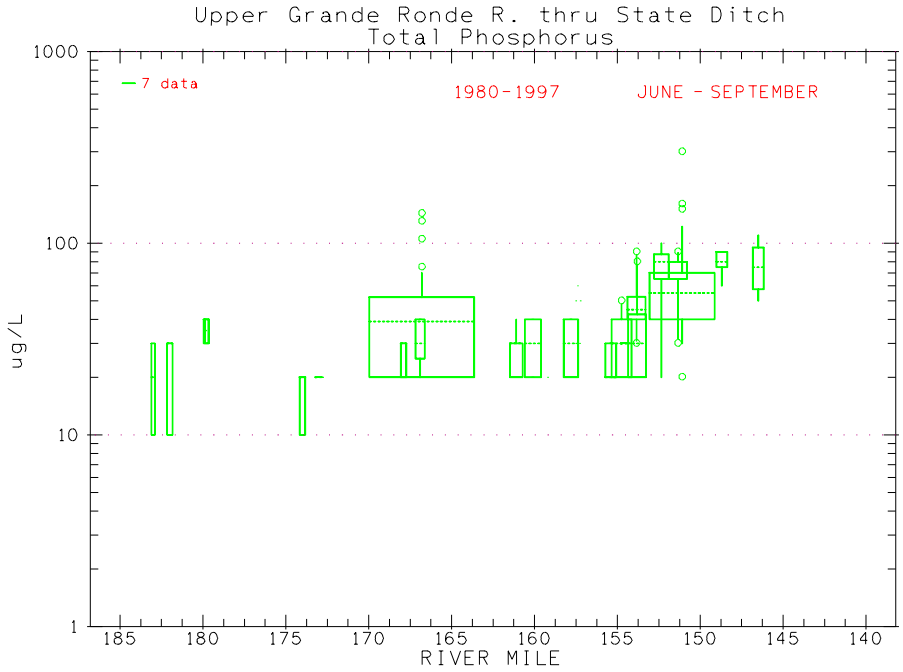

Figure B- 10. Upper Grande Ronde - Total Phosphorus - 1980-1997

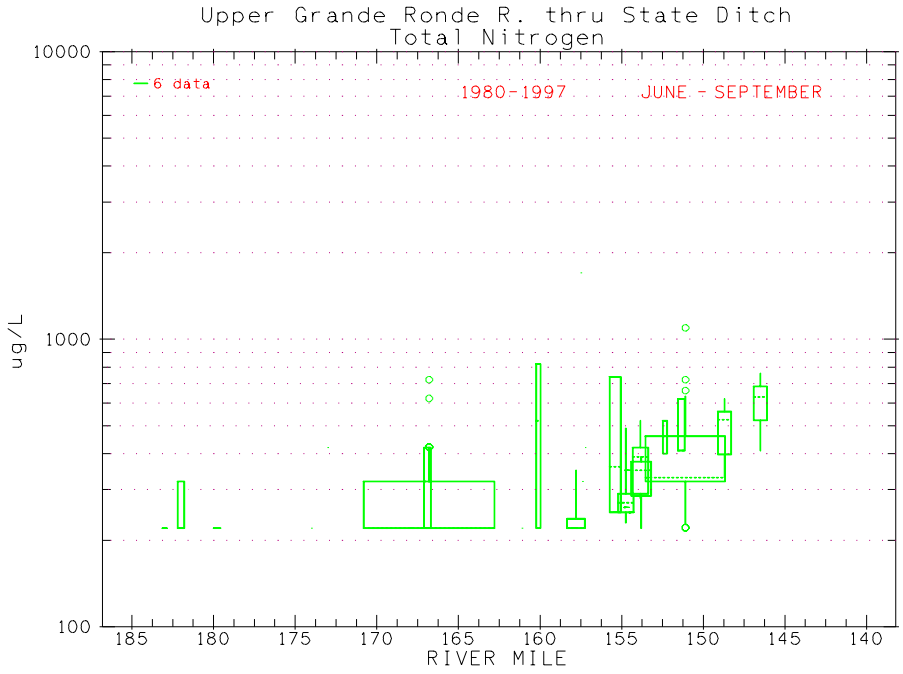

Figure B- 11. Upper Grande Ronde – Total Nitrogen – 1980-1997

Not all nitrogen and phosphorus in a stream is available for algal growth. Total phosphorus (TP) is present in soluble and particulate forms. Soluble reactive phosphorus (SRP) is the phosphorus readily available for algal growth and is quantified by in the laboratory by measuring dissolved orthophosphate. Particulate phosphorus is not readily available for algal growth. Particulate forms include inorganic phosphorus bound to soil particles and particulate organic phosphorus. Note that while particulate phosphorus is not directly available for algal growth, some of it may become available through diagenesis and flux from the sediment.

Total nitrogen (TN) is composed of organic nitrogen, ammonia, nitrite and nitrate. Ammonia, nitrite and nitrate are dissolved inorganic forms which are directly available for algal growth. Organic nitrogen forms are not directly available for algal growth. However, organic nitrogen can potentially become reactive through conversion to ammonia in the benthic layer or water column.

Soluble reactive phosphorus (SRP) is presented in Figure B-12 (SRP quantified by measuring dissolved orthophosphate, as P). SRP concentrations upstream of La Grande are in the 5-25 µg/L range at which some nutrient limitation may occur. Downstream of the La Grande WWTP (~MP 153), the system becomes saturated with SRP relative to algal growth needs. No reduction in SRP concentrations is evident as the water flows downstream.

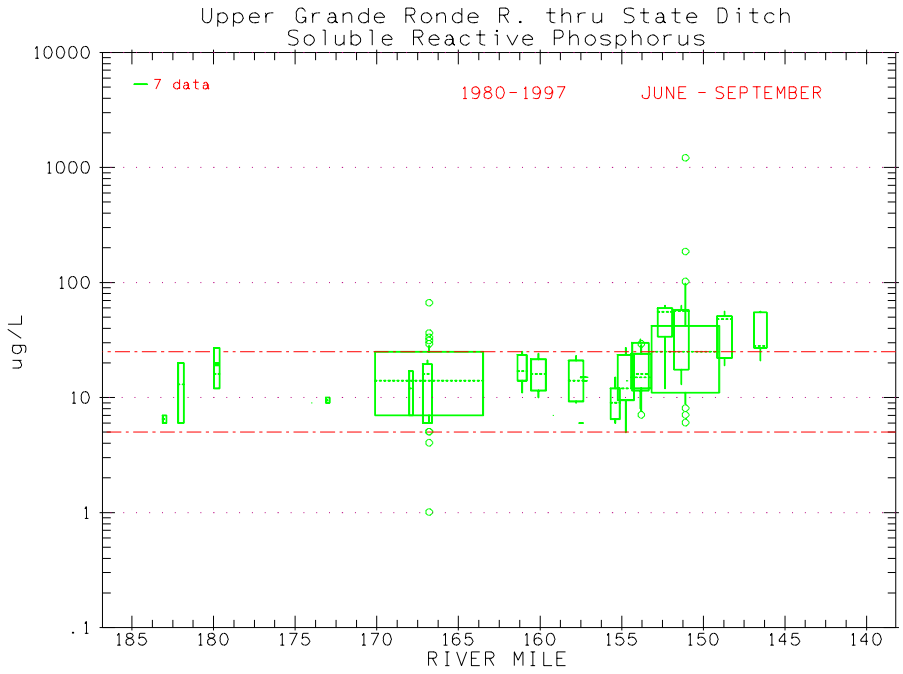

Figure B- 12. Upper Grande Ronde – Soluble Reactive Phosphorus – 1980-1997

Dissolved inorganic nitrogen (DIN) data is presented in Figure B-13. Concentrations upstream of La Grande approach levels at which significant nutrient limitation should occur. Concentrations in this area are frequently less than detection. In the vicinity of La Grande (below MP 155) significant increases in inorganic nitrogen concentrations are observed. Such high concentrations are observed well upstream of the La Grande WWTP, which indicates non-point sources of nitrogen. At the La Grande WWTP further increases are observed. Downstream from La Grande, reductions in DIN are observed, possibly due to uptake by periphyton.

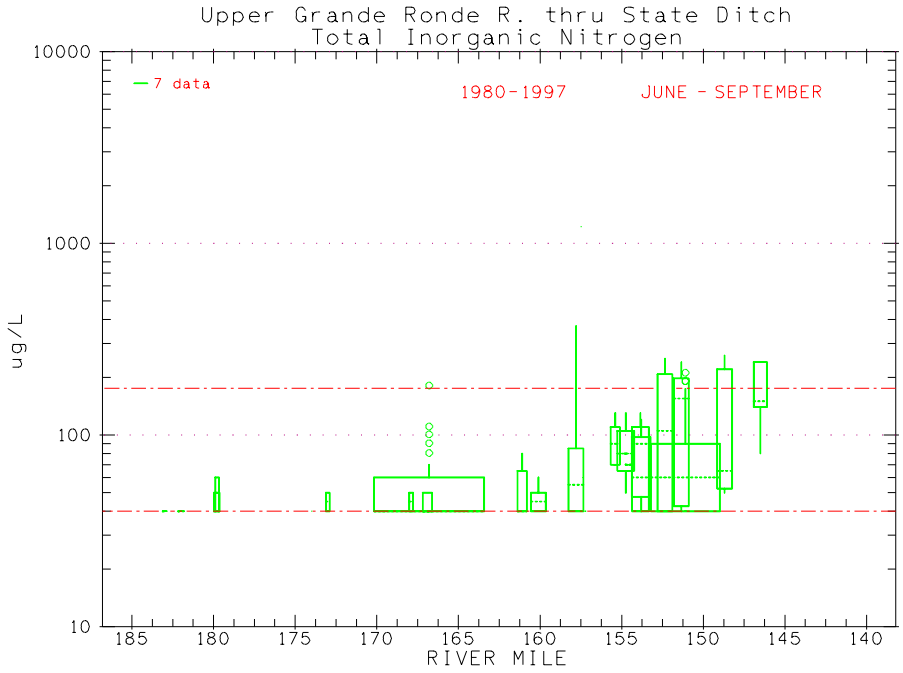

Figure B- 13. Upper Grande Ronde – Total Inorganic Nitrogen – 1980-1997

The ratio of nitrogen to phosphorus is also of interest because it provides insight into which nutrient is limiting algal growth, if any. Algal growth is limited by the nutrient in lowest supply relative to algal cell needs. Under nutrient saturated conditions, algal stoichiometry is generally well represented by the Redfield ratios (HydroQual, 1995):

106C:16N:1P (atomic basis)

which results in a mass basis ratio of N/P of 7. Therefore, the half-saturation constant for nitrogen is 7 times the phosphorus half-saturation constant. Since the ratio of nitrogen to phosphorus in algal cells is about 7 to 1 on a mass basis, if the ratio of water column nitrogen to water column phosphorus is much less than 7, nitrogen is likely to be limiting. However if the N/P ratio is much greater than 7, phosphorus is likely to be limiting. Note that if both nutrients are present in concentrations well in excess of algal needs, then neither would be limiting. Therefore, N/P ratios must be considered in tandem with in-stream concentrations of SRP and DIN. Since algal cell stoichiometry is somewhat variable, in practice, if the N/P ratio is less than 5, nitrogen is considered the limiting nutrient. If greater than 20, phosphorus is the limiting nutrient (Thomann and Mueller, 1987).

Figure B-14 presents N/P ratios calculated using total nitrogen and total phosphorus concentrations while Figure B-15 presents ratios calculated using DIN and SRP. The later figures are the best to use since they consider the readily reactive components. As shown, throughout most of the Grande Ronde River the N/P ratio is less than 5, indicating that nitrogen is the limiting nutrient. A review of Figure B-13 shows that DIN, outside of the regions of influence of the WWTP discharges, is at levels where some limitation is expected. Therefore, in these areas the data strongly indicates that nitrogen is the limiting nutrient.

In the areas directly impacted by the La Grande WWTP (in the vicinity of ~MP 153), N/P ratio is much higher. In these areas both nitrogen and phosphorus are available in abundance and neither nutrient is limiting.

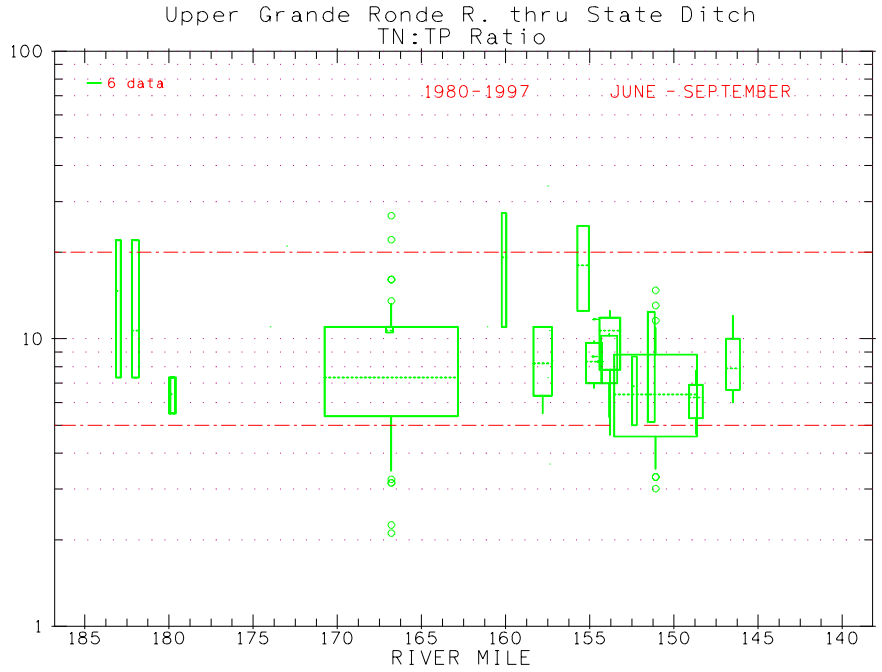

Figure B- 14. Upper Grande Ronde - Total Nitrogen to Total Phosphorus Ratio

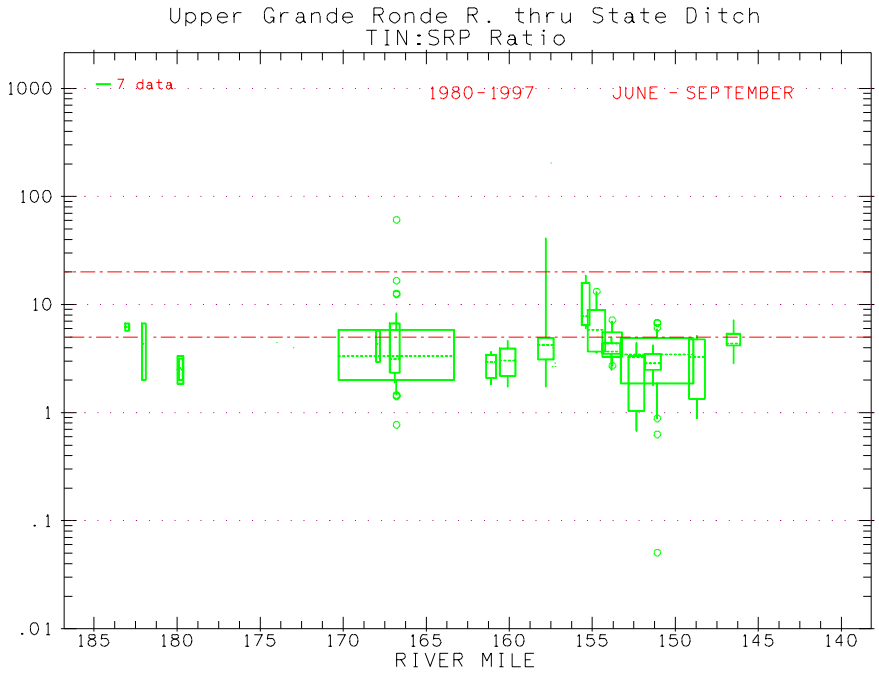

Figure B- 15. Upper Grande Ronde – DIN to SRP Ratio

For the PCM model calibration, typical SRP (via dissolved orthophosphate) and DIN concentrations were estimated for each of the six reaches. The data set used to develop the nutrient inputs was extended beyond the handful of grabs collected during the August 1992 ODEQ water quality survey in order to derive a statistically significant quantity of data. Instead, median concentrations were calculated for each reach using data from mid-July through mid-September for the period of record from 1980 through 1997. The calculated medians for ammonia, nitrite plus nitrate, and SRP, as well as for several other important parameters, are presented in Table B- 4.

Table B- 4. Median Nutrient Concentrations - 1980-1997

Reach	Dissolved Orthophos-phate (µg/L as P)	Ammonia (µg/L as N)	Nitrite + Nitrate (µg/L as N)	BOD_5 (mg/L)	Alkalinity (mg/L as $CaCO_3$)	Turbidity	TSS (mg/L)
4	9.5	<20 (5 of 6 < DL)	<20 (6 of 6 < DL)	0.8	45	1	77.5
5	9.5	20 (1 of 4 < DL)	< 20 (4 of 4 < DL)	0.85	47	2	85
6	10	20 (8 of 29 < DL)	<20 (21 of 29 < DL)	1.1	48	2	86
7	15	20 (10 of 25 < DL)	20 (9 of 25 < DL)	0.9	51	2	86
8	13.5	<20 (20 of 36 < DL)	50 (6 of 36 < DL)	1.6	56	1	89.5
9	28	30 (none < DL)	55 (19 of 42 < DL)	1.6	58	3	97

A summary of critical factors affecting algal activity and observed pH and dissolved oxygen is presented in Table B-5. Comparison of the reach characteristics can provide considerable insight into the system. The definition of effective shade is as follows:

$$\text{Effective Shade} = \frac{(\text{Solar}_1 - \text{Solar}_2)}{\text{Solar}_1}$$

where:

Solar_1 = Potential total daily solar radiation (above trees, etc.)

Solar_2 = Total daily solar radiation at stream surface

Therefore, in a reach with a percent effective shade of 17.5%, 17.5% of the potential solar radiation is attenuated by shade, while 82.5% reaches the stream surface.

As Table B-5 shows, Reaches 8 and 9 have much larger diurnal dissolved oxygen and pH fluctuations than Reaches 4 through 7. The difference appears to be due to the higher nutrient concentrations, solar radiation, and temperature in Reaches 8 and 9. Low reaeration rates in Reaches 8 and 9 are also likely a factor.

Table B- 5. Periphyton related parameters

Reach	Depth (ft)	Effective Shade (%)	Average Temp (^oC)	Max Temp (^oC	Δ Temp (Min to Max) (^oC)	DIN (µg/L)	SRP (µg/L)	Alkalinity (mg/L as $CaCO_{3)}$	K_a^* (1/day)	Δ DO (Min to Max) (mg/L)	Min DO (mg/L)	Δ pH (Min Max) (su)	Max pH (su)
4	0.52	17.5	13.1	18.7	9.9	20	9.5	45	63.3	2.35	8.55	0.95	8.75
5	0.72	7.6	14.4	19.3	9.7	30	9.5	47	30.2	3.55	7.80	1.45	9.25
6	0.72	6.5	16.1	20.2	8.4	35	10	48	19.0	3.1	7.75	1.15	9.05
7	0.72	9.8	14.7	18.3	7.6	40	15	51	32.0	2.85	7.9	1.10	9.00
8	0.81	0.11	16.74	20.3	6.9	65	13.5	56	14.0	9.2	6.35	2.1	9.45
9	0.92	0.00	16.15	20.8	9.05	85	28	58	12.8	13.3	5.65	2.60	10.3

* K_a estimated as function of velocity and depth via the Owens equation.
Observed temperature, DO and pH shown in table via averaging data from two Hydrolabs for each reach.
Δ indicates range from daily minimum to daily maximum.

4.5 Observed Periphyton Data

Periphyton data was collected on the Grande Ronde River by DEQ in August, 1992. Data was collected at 8 stations for three parameters: chlorophyll a, pheophyton, and ash free dry weight. Two techniques were utilized: natural rock scrapings and artificial substrate sampling (Surber).

Observed chlorophyll a data is presented in Table B-6 and Figure B-16.

Table B- 6. Rock Scrapings - Chlorophyll a

Station	MP	n	Mean	Std.Dev.	95% Confidence Interval Range
404506	182	8	38.1	13.2	27.1-49.1
404505	176	5	65	32.5	24.6-105.4
404359	167	5	43.4	29.1	7.3-79.5
404357	160	5	42.4	24.6	11.9-72.9
404354	154.75	5	123.0	95.	5-240
404353	153.85	5	65.2	38.7	17.1-113.3
404507	153.75	5	198.6	133.1	33.4-363.8
404356	150.1	5	80.6	55.5	11.7-149.5

As shown in Table B-6, the 95% Confidence Intervals are quite large, indicating the large variability in the observed concentrations at each station and the relatively small sample sizes. Due to this large variability, only limited insight can be derived from the data, but the data does suggest increasing algal concentrations in the downstream direction.

The upper panels of Figure B-16 present data from rock scrapings and the lower panels data from artificial substrate sampling (note the difference in scale between the rock scrapings and the surber samples). The panels on the left show all the data from MP 182 to MP 150, while the panels on the right are “blowups” which present only the data from MP 155 to MP 150 in order to better evaluate the impact of the LaGrande WWTP discharge at MP 153.8.

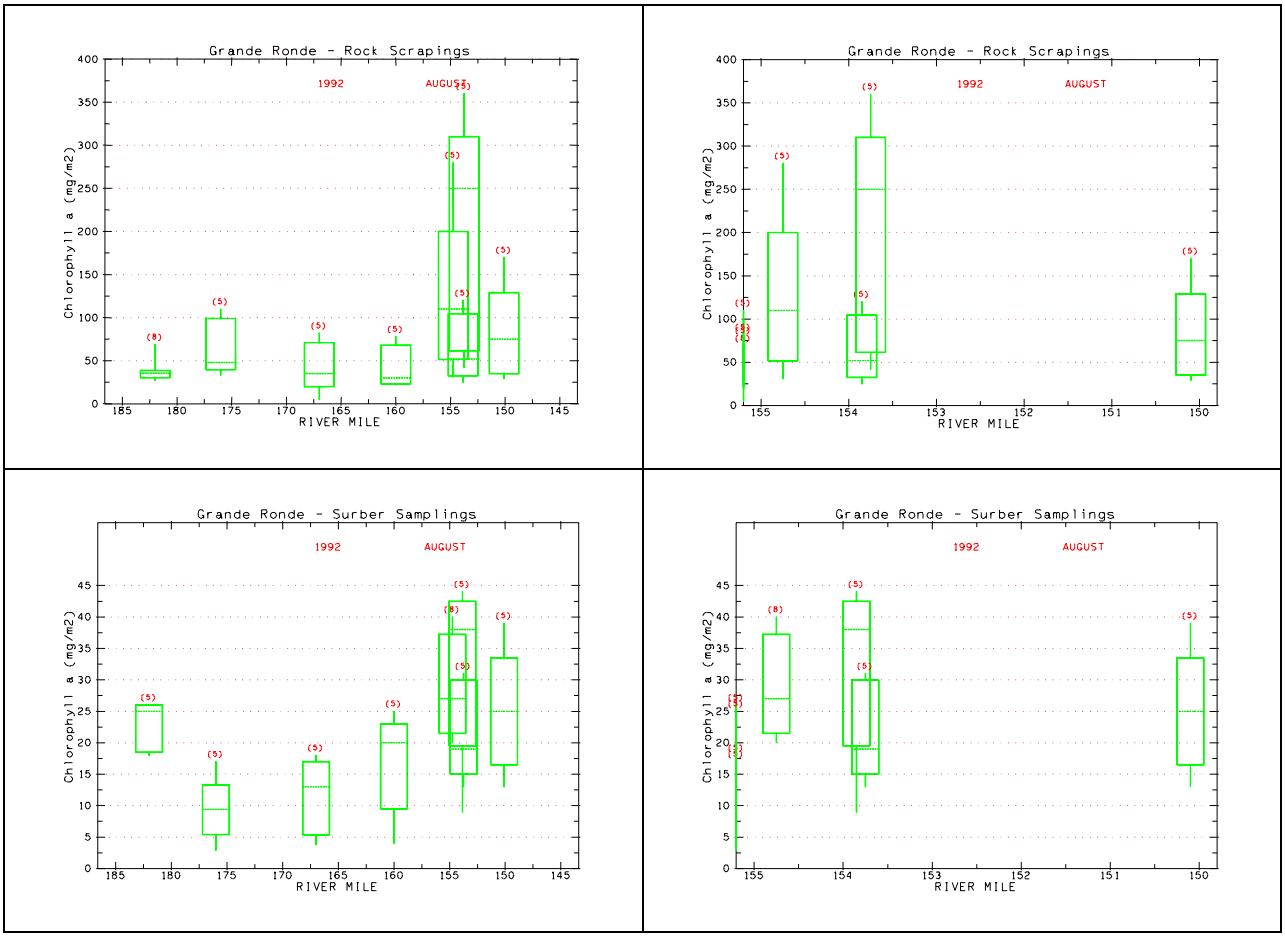

Figure B- 16. Chlorophyll a from rock scrapings and artificial substrate sampling

As shown, mean chlorophyll a concentrations increase in a downstream direction. Chlorophyll a concentrations are significantly greater in the Grande Ronde Valley than at upstream stations.

Comparison of chlorophyll a concentrations from rock scrapings to concentrations from artificial substrate show that chlorophyll a concentrations on rocks were 1.6 to 9.0 times greater than on the Surber samplers. This may be because Surber samplers, which provide a reasonable estimate of filamentous algae, typically grossly underestimate the amount of diatoms and other smaller algae in a stream. Another possibility is that a much of chlorophyll a on the rocks may be inactive.

Rock scrapings show a dramatic increase in mean chlorophyll a downstream of the LaGrande WWTP. The mean concentration just upstream of the WWTP (MP 153.85) is 65 mg/m^2 and just downstream of the discharge (MP 153.75) is 199 mg/m^2. This increase was found to be statistically significant. However, the artificial substrate samplings do not show an increase due to the WWTP, but rather a decrease in mean concentrations from 32 mg/m^2 upstream of the discharge to 22 mg/m^2 downstream of the discharge, although this decrease was not found to be statistically significant.

Observed ash free dry weight data from the same samples is presented in Figure B-17, and a third indicator of periphyton mass, pheophytin, is presented in Figure B-18. Pheophyton concentrations (Figure B-18) increase significantly in the valley. ADFW concentrations (Figure B-17) do not show conclusive trends.

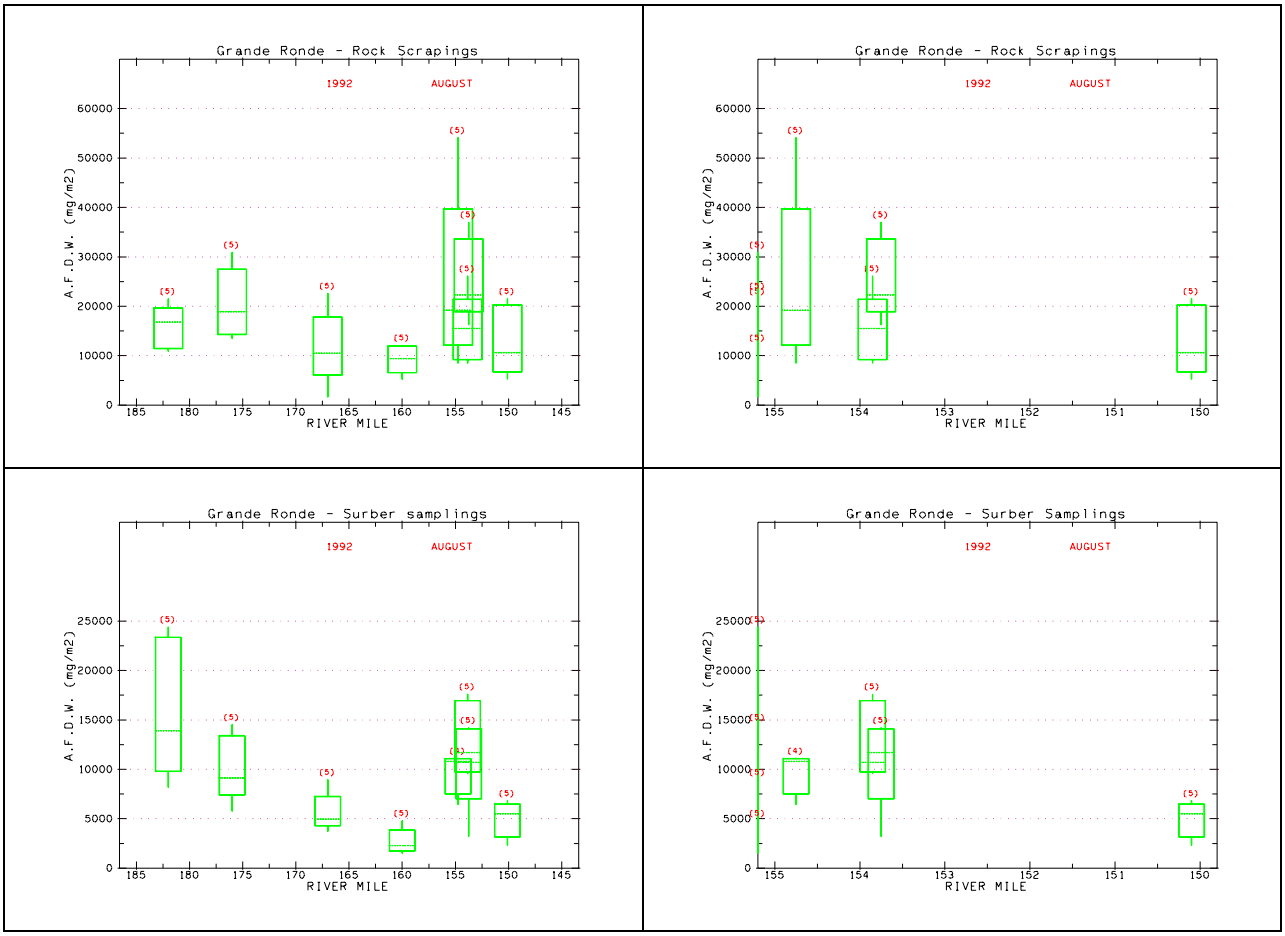

Figure B- 17. Ash free dry weight from rock scrapings and artificial substrate sampling

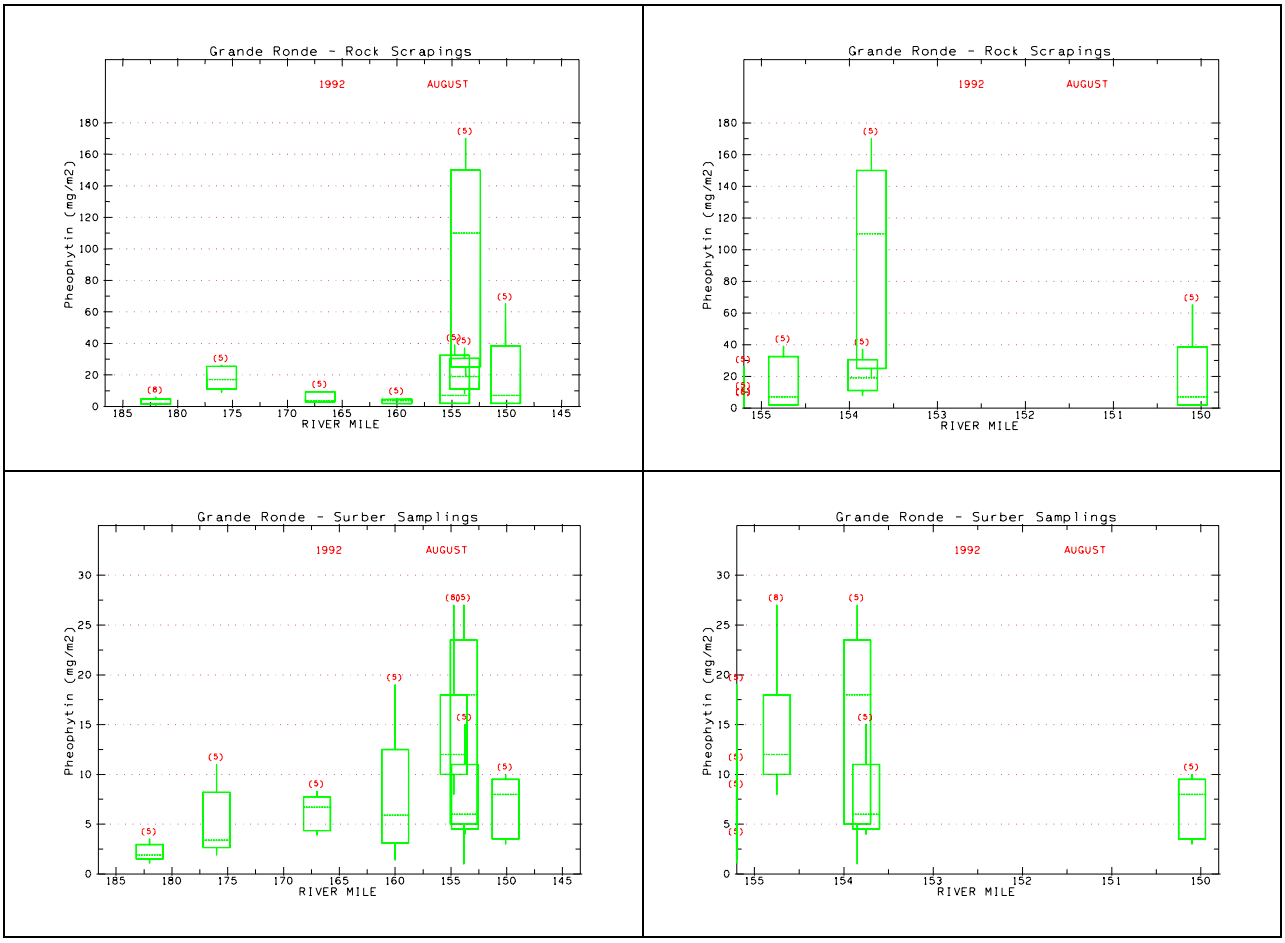

Figure B- 18. Pheophytin from rock scrapings and artificial substrate sampling

4.6 Heat Source Calculations

A model of the Grande Ronde was developed using the temperature model Heat Source and calibrated for August 25, 1992 (Boyd, 1996; ODEQ 1999). The calibrated Heat Source model provided the river geometry (width and depth), flow rates, velocity, hourly solar radiation estimates, and hourly temperature estimates. Model calculated vs. observed temperature plots for the six reaches for August 25, 1992 are presented in Figure B-19.

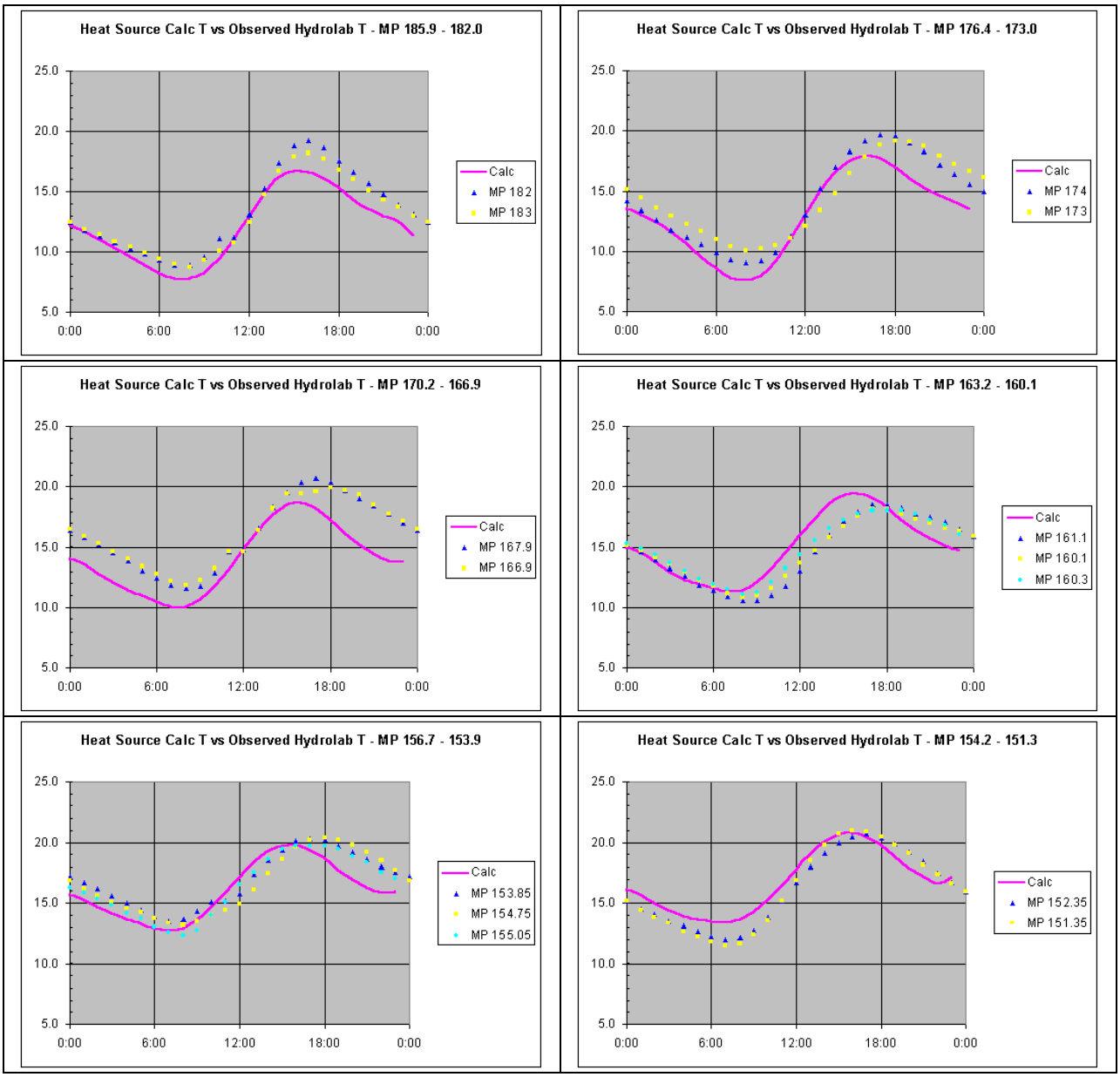

Figure B- 19. Model calculated vs. observed temperature

The solid lines are model calculated temperatures, while the single sets of data points are observed temperatures. For each reach, data was collected using two Hydrolab datasondes spaced one mile apart. In addition, several reaches each had additional temperature datasondes. For three of the reaches Hydrolab data was available for August 26, but not for August 25 (reaches 185.9-182.0, 170.2-166.9, and 156.7-153.9). For these the August 26 data is plotted. As shown, Heat Source generally provided accurate predictions of temperature.

Temperatures and solar radiation entering the river calculated by the Heat Source models were fed into the PCM model to calculate pH and dissolved oxygen concentrations.

4.7 PCM Calibration Parameters

PCM was calibrated using the observed Hydrolab pH and dissolved oxygen data. The same model calibration parameters were applied to all six modeled reaches. Model parameters are presented in Table B-7.

Table B- 7. PCM Model Parameters

Parameter	Value	Units
Maximum algal growth rate at 20 C, $G_{\max}$	1.8	1/day
Michaelis-Menton half-saturation constant for phosphorus, $K_{m,phos}$	4	µg/L
Michaelis-Menton half-saturation constant for nitrogen, $K_{m,nitr}$	28	µg/L
Saturating light intensity, I_s	350	Ly/day
Photosynthetically active fraction of solar radiation, PARfrac	0.43	
Exponent for Walker modified Steele formulation for solar radiation inhibition, PARwalker	0.8	
Factor to convert Oxygen reaeration rate to CO2 aeration rate, KacFac	0.923	
Partial pressure of CO2 in atmosphere, pCO2	0.000355	atm
BOD decay rate coefficient at 20°C, $K_{d,20^oC}$	0.5	1/day
Moles of O2 produced per mole of algal C produced for ammonia as the N source, A_{oc,NH_4N}	1	
Moles of O2 produced per mole of algal C produced for nitrate as the N source, A_{oc,NO_3N}	1.3019	
Equivalents of alkalinity produced per mole of algal C produced for ammonia as N source, a_{AlkC,NH_4N}	-0.13208	Eq/mole
Equivalents of alkalinity produced per mole of algal C produced for ammonia as N source, a_{AlkC,NO_3N}	0.169811	Eq/mole
Moles water column C consumed per mole algal C produced, $a_{wcCa\lg C}$	0.5	
algal cell carbon to chlorophyll a ratio (mass basis), a_{CChl}	75	
Temperature correction coefficient (theta) for reaeration, θ_{K_a}	1.024	
Temperature correction coefficient for respiration (for calculation of daytime respiration from nighttime respiration), θ_{K_a}	1.047	
Temperature correction coefficient for algal respiration θ_{DP}	1.047	
Temperature correction coefficient (theta) for algal growth, θ_{GP}	1.066	
Factor to adjust calculated daily average periphyton mass (1.0 for no adjustment), PeriAdjust	1	
Factor to adjust elevation to account for atmospheric pressure (1.0 for no adjustment), ElevAdjust	1	
Factor to increase or decrease Ka for all reaches from that calculated, KaAdjust	1	
Factor to increase or decrease light extinction coef Ke, KeAdjust	1	
Factor to increase or decrease calculated nighttime respiration at 20°C, RespAdjust	1.1	
Slope from correlation of PeriMA on GPavg (from 6 reaches), PeriSlope	29.006	

4.8 Model Calibration using observed temperatures

Initial PCM calibration was performed using the observed Hydrolab temperatures and calculated Heat Source solar radiation. Observed temperatures were used to minimize carryover of model imprecision from model to model. Note that this option is not available for solar radiation, since solar radiation observations are not available, so Heat Source calculated solar radiation was used. Resultant pH and DO calculations versus observations are presented in Figures B-20 and B-21.

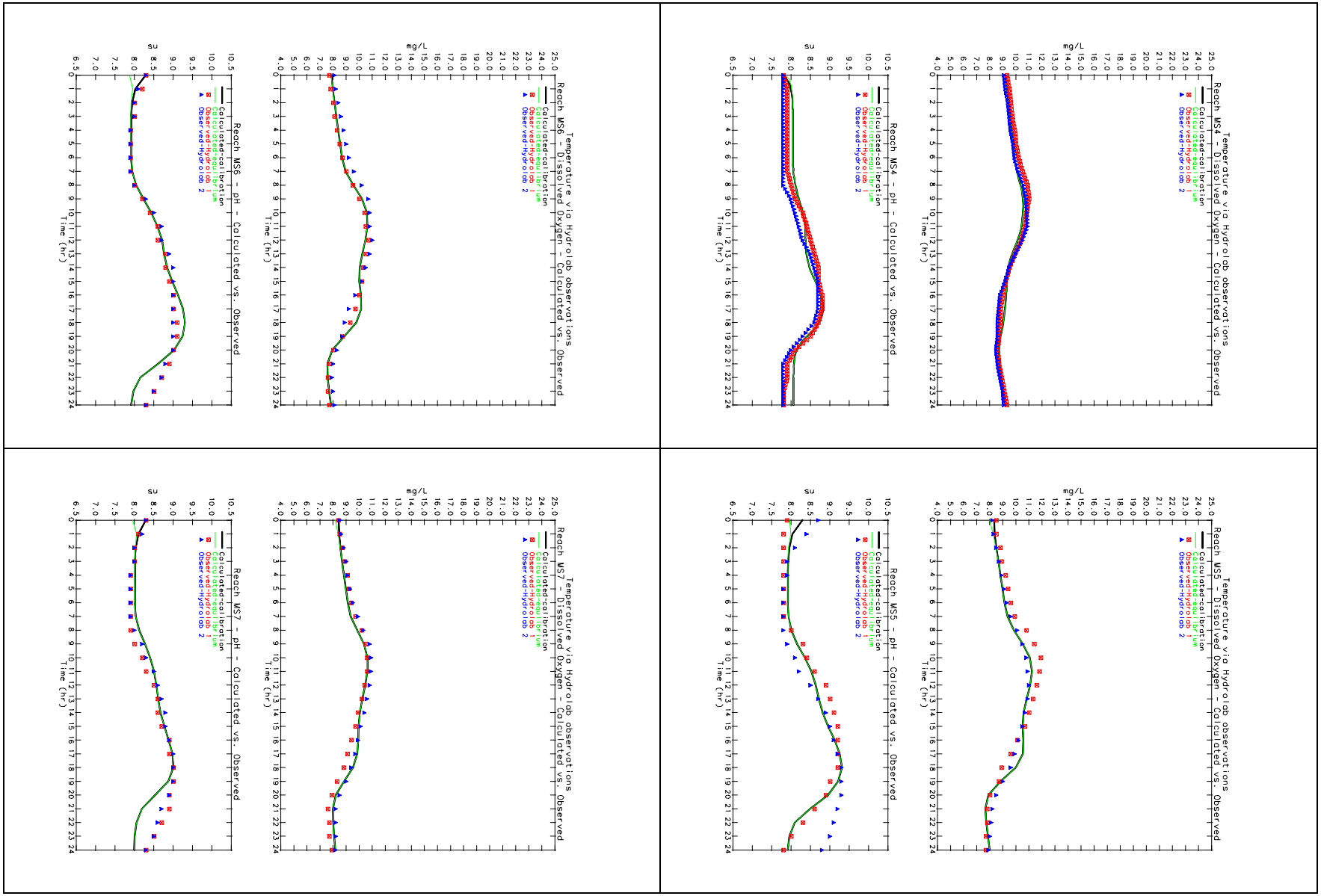

Figure B- 20. Calculated pH and DO vs. observations - Temperature via observations (above MP 160)

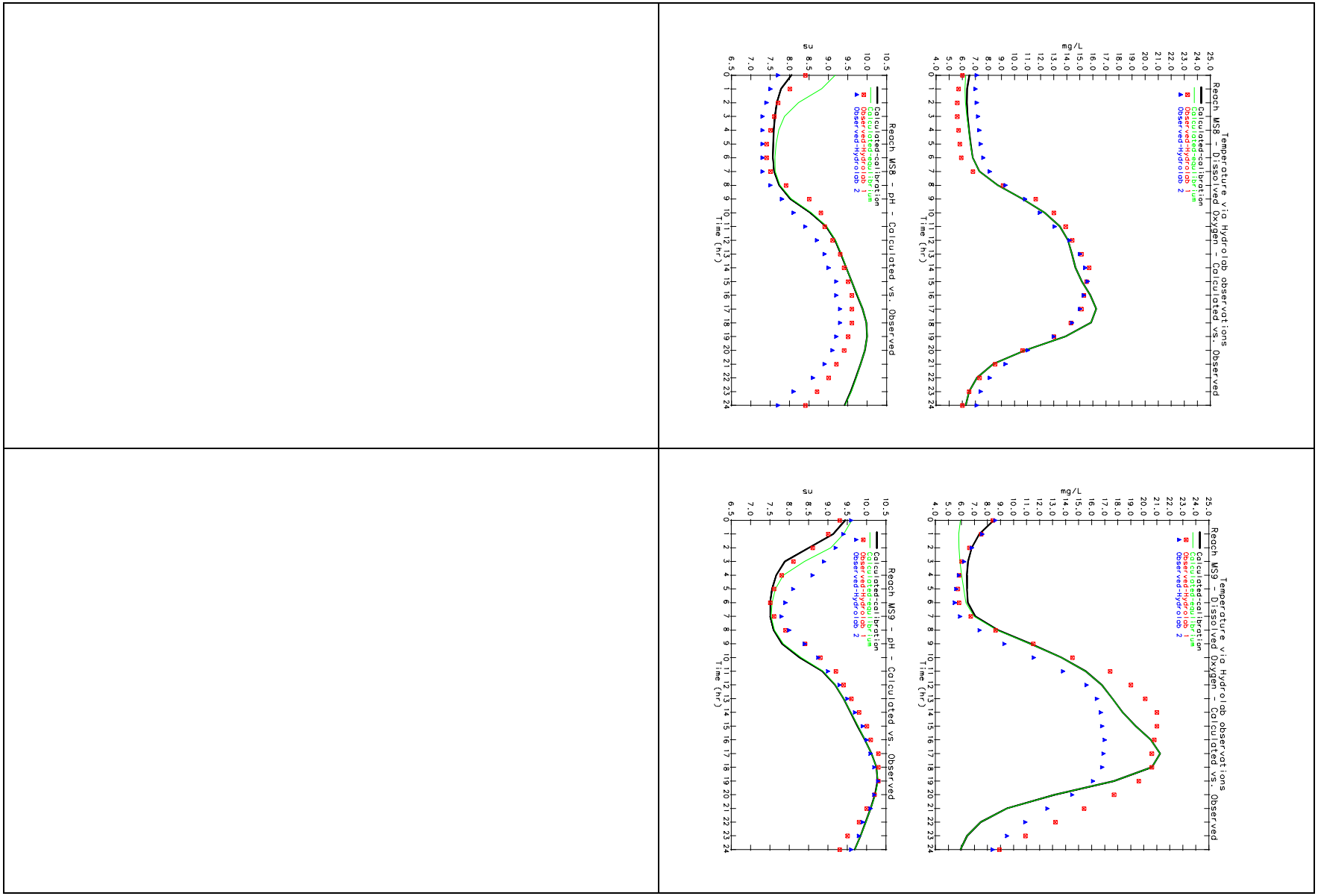

Figure B- 21. Calculated pH and DO vs. observations - Temperature via observations (below MP 160)

The solid lines in Figures B-20 and B-21 are PCM calculated dissolved oxygen and pH, while the data points are Hydrolab observed concentrations (2 Hydrolabs per reach). The thicker lines shown are calculated concentrations using the initial pH and DO concentrations at midnight as the initial values. Since for simulations initial concentrations would generally not be know, the model was run iteratively until concentrations became stable. These calculated equilibrium concentrations are shown by the thinner lines. In general, there was little difference between equilibrium and calibration concentrations, which indicates the model can be applied to conditions other that calibration conditions.

In Table B-8 are presented the growth rate, G_P; death/respiration rate, D_P; death/respiration rate at 20^oC; sloughing rate, F_{slough}; and periphyton mass calculated by PCM for each reach. As shown, growth rate increases in a downstream direction, due to increases in nutrient concentrations, light, and temperature. Calculated periphyton mass concentrations also increase in a downstream direction. Periphyton concentrations are provided in Table B-8 in three formats, carbon per unit volume, carbon per unit benthic area, and chlorophyll a per unit benthic area. Model calculations are performed in terms of carbon. Since the ratio of carbon to chlorophyll a in the Grande Ronde is unknown, a range is given in the table based on literature ratios of 50-100 g carbon per g chlorophyll a. Note that calculated periphyton concentrations are within the range of the observed concentrations from rock scrapings described in Section 4.5 above.

Table B- 8. Calculated growth, death/respiration, and sloughing rates and periphyton mass

Reach	Gpavg	DPavg	DP20	Fslough	Average Periphyton Mass		
	(1/day)	(1/day)	(1/day)	(1/day)	gC/m3	gC/m2	mg Chlorophyll a /m2
4	0.2153	0.0617	0.0846	0.1536	34.44	5.518	55-110
5	0.2673	0.1735	0.2253	0.0938	36.109	7.968	80-159
6	0.3399	0.2299	0.2748	0.11	29.511	6.533	65-131
7	0.323	0.2482	0.3175	0.0748	21.61	4.745	47-95
8	0.4574	0.2649	0.3079	0.1925	40.011	9.833	98-197
9	0.5003	0.2495	0.2976	0.2508	55.761	15.645	156-313

Of primary concern is the model's ability to accurately calculate minimum daily DO and maximum daily pH, since these are what water quality standards are based upon. Calculated concentrations are compared to observations in Table B-9. In the table, both the calibration and equilibrium concentrations are shown, as well as the observed minimum DO and maximum pH from both Hydrolabs from each reach. As shown, the model provided reasonable predictions of both minimum DO and maximum pH.

Table B- 9. Calculated pH and DO concentrations vs. observations

	Dissolved Oxygen				PH				delta	delta
	Calc Min	Equi min	Obs1 min	Obs2 min	Calc max	Equi max	Obs1 Max	Obs2 Max	DO calc	DO obs
4	8.7	8.7	8.61	8.51	8.82	8.82	8.8	8.7	1.87	2.33
5	7.72	7.72	7.7	7.95	9.29	9.29	9.2	9.3	3.47	3.53
6	7.6	7.6	7.6	7.95	9.28	9.28	9.1	9	3.02	2.97
7	8.02	8.02	7.65	8.2	9	9	9	9	2.63	2.83
8	6.36	6.23	5.6	7.05	9.99	9.99	9.6	9.3	9.7	9.2
9	6.19	5.82	5.75	5.55	10.27	10.28	10.3	10.25	14.76	13.25

Statistics describing model accuracy and precision are presented in Table B-10. The statistics presented describe how well calculated concentrations compared with observed concentrations at each time step throughout the day.

Table B- 10. Model accuracy and precision (temperature via observations)

	Average Error (mg/L)				Relative error (%)				Standard error of the estimate (mg/L)			
	DO Calc	DO Equi	pH Calc	pH Equi	DO Calc	DO Equi	pH Calc	pH Equi	DO Calc	DO Equi	pH Calc	pH Equi
4	-0.03	-0.03	0.11	0.11	1.9	1.9	1.8	1.8	0.22	0.22	0.16	0.16
5	-0.08	-0.1	-0.06	-0.08	2.8	3	1.8	2	0.34	0.35	0.22	0.23
6	-0.06	-0.06	-0.04	-0.06	2.3	2.4	1.5	1.8	0.28	0.28	0.2	0.22
7	-0.04	-0.05	-0.05	-0.07	2.1	2.3	1.8	2	0.24	0.25	0.23	0.24
8	-0.04	-0.07	0.37	0.51	3.7	3.9	4.5	6.1	0.56	0.56	0.52	0.63
9	-0.31	-0.58	-0.16	-0.08	10.7	11.9	2.3	2	1.89	1.98	0.28	0.22

A second set of statistics was calculated to indicate how well calculated daily minimum DOs and maximum pHs compared with observed minimums and maximums. These are presented in Table B-11. While Table B-10 indicates how well the lines in Figure B-21 match the data points, Table B-11 indicates how well calculated the calculated daily minimum and maximums presented in Table B-9 match observed daily minimums and maximums. As Table B-11 shows, the model provides acceptable levels of accuracy and precision.

Table B- 11. Summary statistics (temperature via observations)

Average Error: minimum DO= 0.0142 mg/L maximum pH= 0.1440 su (if > 0 overpredicts, if < 0 underpredicts)
Relative Error: minimum DO= 1.7845 % maximum pH= 1.6310 % (smaller is better)
Std Errors of the Estimate: minimum DO= 0.1336 mg/L maximum pH= 0.2429 su (estimate of precision, smaller is better)

4.9 Model Calibration using Heat Source calculated temperatures

The above analysis was repeated using Heat Source calculated temperatures, rather than observed temperatures. Since temperature model predictions must be used to provide temperature and solar radiation inputs for predictive scenarios, the accuracy of this second calibration analysis is more important than the above. As shown in Figures B-22 and B-23, pH and DO predictions using Heat Source calculated temperatures also closely match the observations.

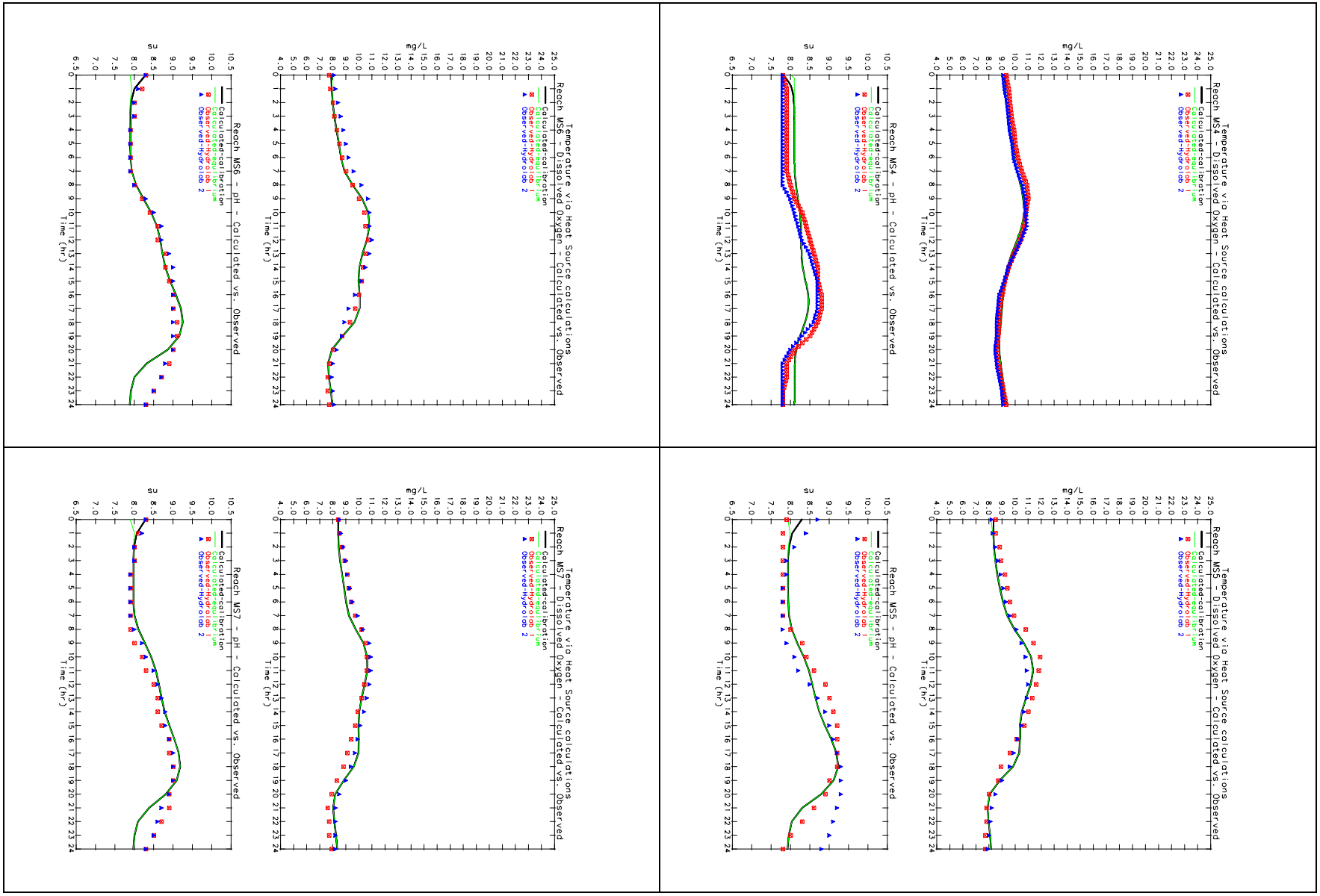

Figure B- 22. Calculated pH and DO vs. observations - Temperature via model (above MP 160)

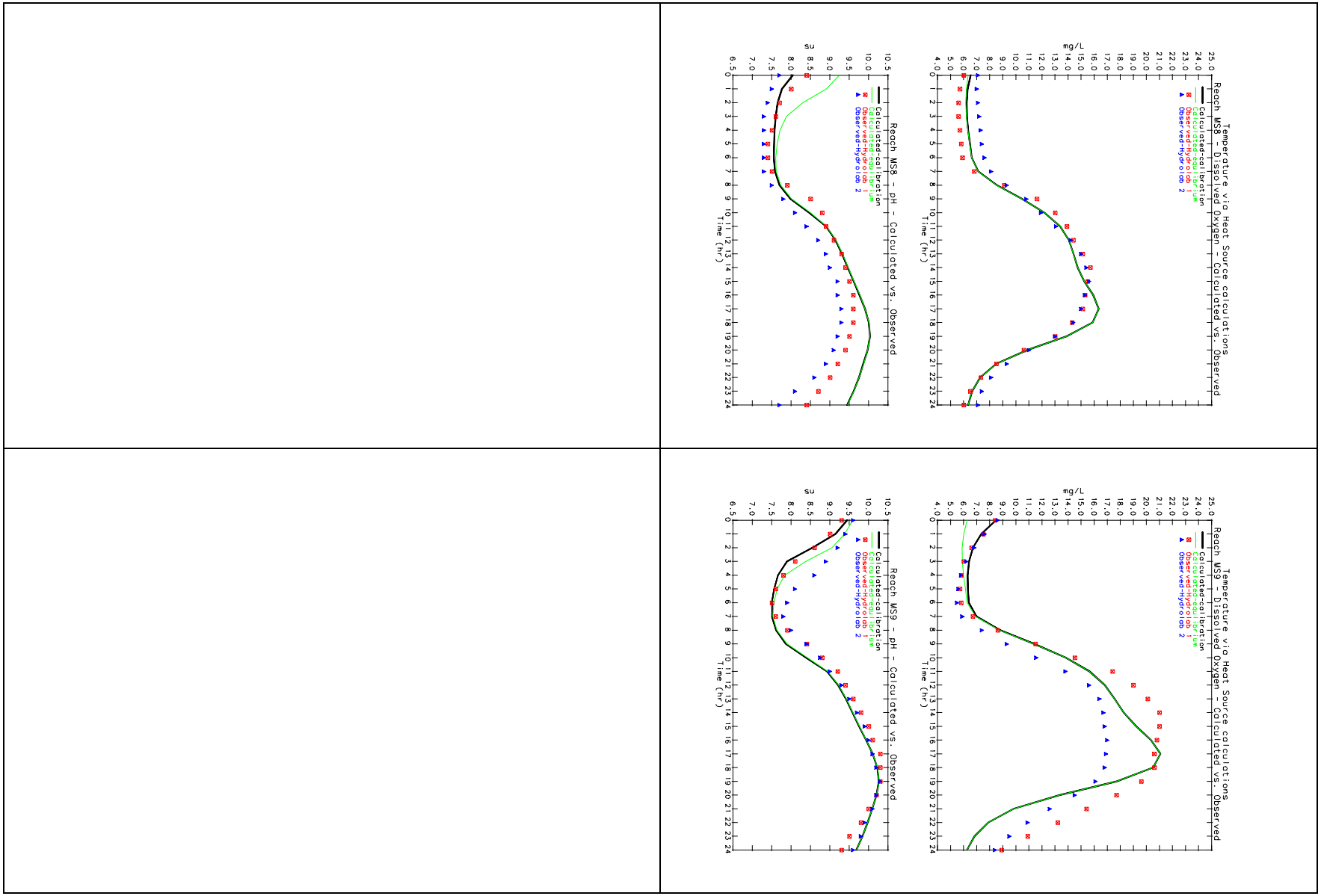

Figure B- 23. Calculated pH and DO vs. observations - Temperature via model (below MP 160)

Calculated minimum and maximum concentrations are compared to observations in Table B-12. As shown, calculations using Heat Source for temperature are nearly as accurate as those using observed temperatures (Table B-10).

Table B- 12. Model accuracy and precision (temperature via model)

	Dissolved Oxygen				pH				delta	delta
	Calc Min	Equi Min	Obs1 min	Obs2 min	Calc max	Equi max	Obs1 Max	Obs2 Max	DO calc	DO obs
4	8.8	8.8	8.61	8.51	8.47	8.47	8.8	8.7	1.89	2.33
5	7.95	7.95	7.7	7.95	9.21	9.21	9.2	9.3	3.37	3.53
6	7.69	7.69	7.6	7.95	9.24	9.24	9.1	9	3.09	2.97
7	8.08	8.08	7.65	8.2	9.17	9.17	9	9	2.57	2.83
8	6.26	6.2	5.6	7.05	10.02	10.03	9.6	9.3	9.89	9.2
9	6.33	5.91	5.75	5.55	10.25	10.26	10.3	10.25	14.48	13.25

Summary statistics for these model runs are presented in Table B-13. As shown, the model provides acceptable levels of accuracy and precision.

Table B- 13. Summary statistics (temperature via model)

Average Error: minimum DO= 0.1058 mg/L maximum pH= 0.0956 su (if > 0 overpredicts, if < 0 underpredicts)
Relative Error: minimum DO= 2.3907 % maximum pH= 2.3237 % (0-100%, smaller is better)
Std Errors of the Estimate: minimum DO= 0.1880 mg/L maximum pH= 0.2829 su (estimate of precision)

In order to correct for the slight amount of model inaccuracy when comparing calculated concentrations to standards, calculated daily maximum pHs and minimum DOs are corrected in the following manner:

$$\text{Correction Factor} = \frac{\text{Calibration Calculated Equilibrium Min DO}}{(\text{Observed min DO}_1 + \text{Observed min DO}_2)/2}$$

$$\text{Corrected Simulation DO} = \frac{\text{Simulation Calculated DO}}{\text{Correction Factor}}$$

4.10 Correlation of Periphyton Mass with Algal Growth Rate

Figure B-24 shows the correlation between periphyton mass and daily average growth for the August 25 calibration scenario.

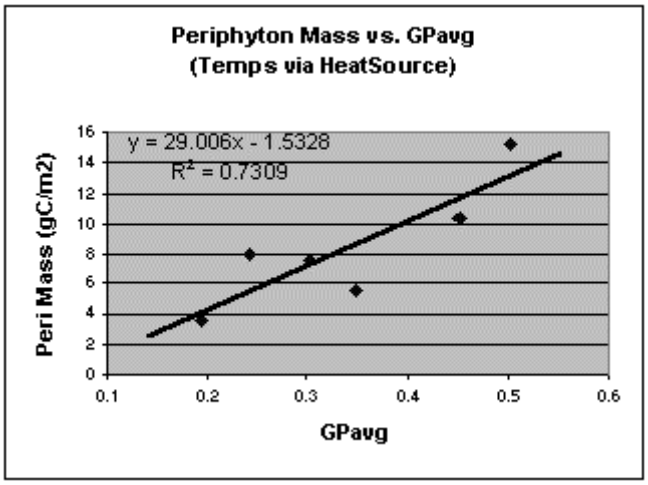

Figure B- 24. Correlation between periphyton mass and growth rate

As shown, the r^2 for this the correlation is 0.73, which shows that periphyton mass is strongly correlated with growth rate. This relationship is very useful for projections as it allows periphyton mass to be revised as a function of growth rate.

4.11 Methodology for performing modeling simulations

With calibrated temperature and periphyton models, diel pH and DO can be estimated for a variety of riparian, flow, width, depth and nutrient scenarios. The following steps are followed when performing simulations:

1) The temperature model is run with desired riparian vegetation, flow, and active and wetted channel characteristics,
2) Solar radiation and river temperatures calculated by the temperature model are input to the PCM model,
3) New algal growth rates corresponding to the desired simulation condition (increased shade, reduced nutrients, etc.) are calculated by PCM.
4) PCM uses the slope of the linear regression line from the mass to growth rate correlation to estimate new periphyton masses corresponding to the new algal growth rates (see dashed slope line on Figure B-25).

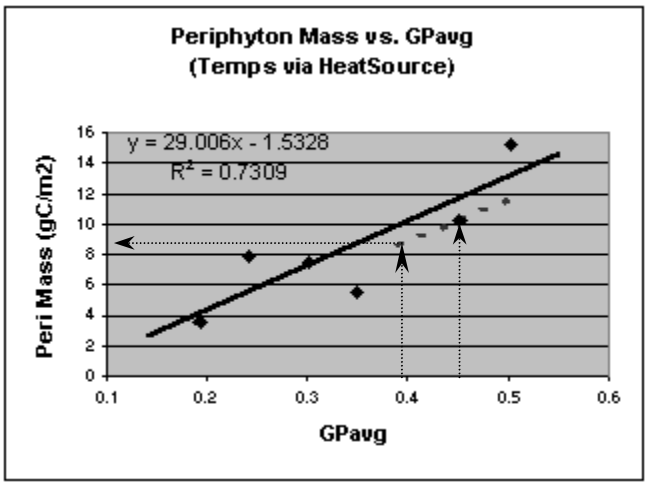

Figure B- 25. Method for estimating periphyton mass from growth rate

For example, a modeling scenario in which shade is increased may reduce the daily average growth rate in a reach from 0.45/day to 0.40/day. The periphyton mass corresponding to the 0.45/day growth rate was calculated to be 10.3 g C/m^2 for calibration conditions. To calculate a new periphyton mass for the increased shade scenario, PCM extrapolates along the dashed line in Figure B-25 to a new mass of 8.5 g C/m^2.

5) New algal death/respiration rates are calculated by PCM as functions of calibration D_P at 20^{o}C and revised temperatures.
6) Diel pH and DO are calculated.

5 Simulations and Load Allocations

A series of simulations were performed for various shade and nutrient concentration reduction scenarios to derive nutrient load allocations. Modeling was performed for conditions which occurred on August 25, 1992. This date was selected to take advantage of the extensive continuous monitoring data which is available from August 24 through August 27, 1992. This should be a worst case or near worst case scenario, since the most serious pH and DO standards violations tend to occur in August, and since flow rates during August 1992 were lower than during a typical August. Flow rates in the Grande Ronde for this period were less than 17 cfs in the Valley and were similar to the 7Q10 river flow rate of 14 cfs. (7Q10 is the once in 10 year 7-day average low flow rate. The 7Q10 is the flow rate most commonly used in the U.S. for setting load allocations (Stedinger, et al, 1993.)

5.1 Current Riparian Condition Scenarios

Modeling was performed using current riparian conditions with nutrient concentration reductions of 0%, 30%, 50% and 70% in order to estimate load reductions needed to meet for current riparian conditions. Stream temperature and effective shade for each scenario is shown in Table B-14. Also shown in Table B-14 are current nutrient concentrations for the late summer calibration period.

Table B- 14. Model inputs for current riparian condition scenarios

Reach	Depth (ft)	Effective Shade (%)	Average Temp (°C)	Max Temp (°C	ΔTemp (°C)	DIN (µg/L)	SRP (µg/L)
4	0.52	17.5	12.1	16.7	4.3	20	9.5
5	0.72	7.6	13.0	18.0	10.3	30	9.5
6	0.72	6.5	14.0	18.6	8.6	35	10
7	0.72	9.8	15.1	19.4	8.1	40	15
8	0.81	0.11	16.0	19.8	7.0	65	13.5
9	0.92	0.00	16.7	20.8	7.46	85	28

Calculated pH and DO for current riparian conditions for nutrient reductions of 0%, 30%, 50% and 70% are presented in Figures B-26 and B-27. Also shown are the applicable standards (dashed lines).

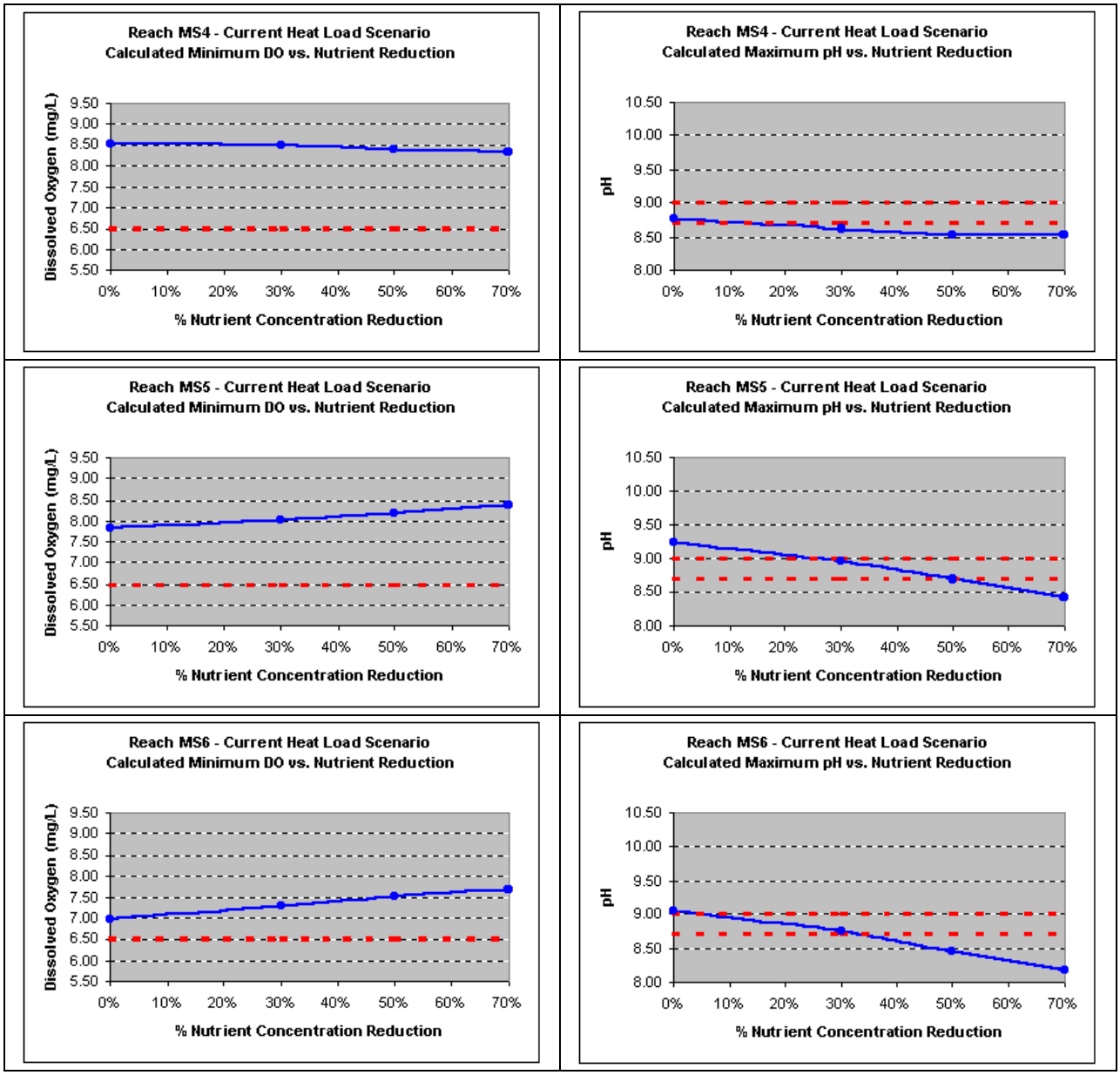

Figure B- 26. Calculated pH and DO for current riparian conditions for various nutrient reductions

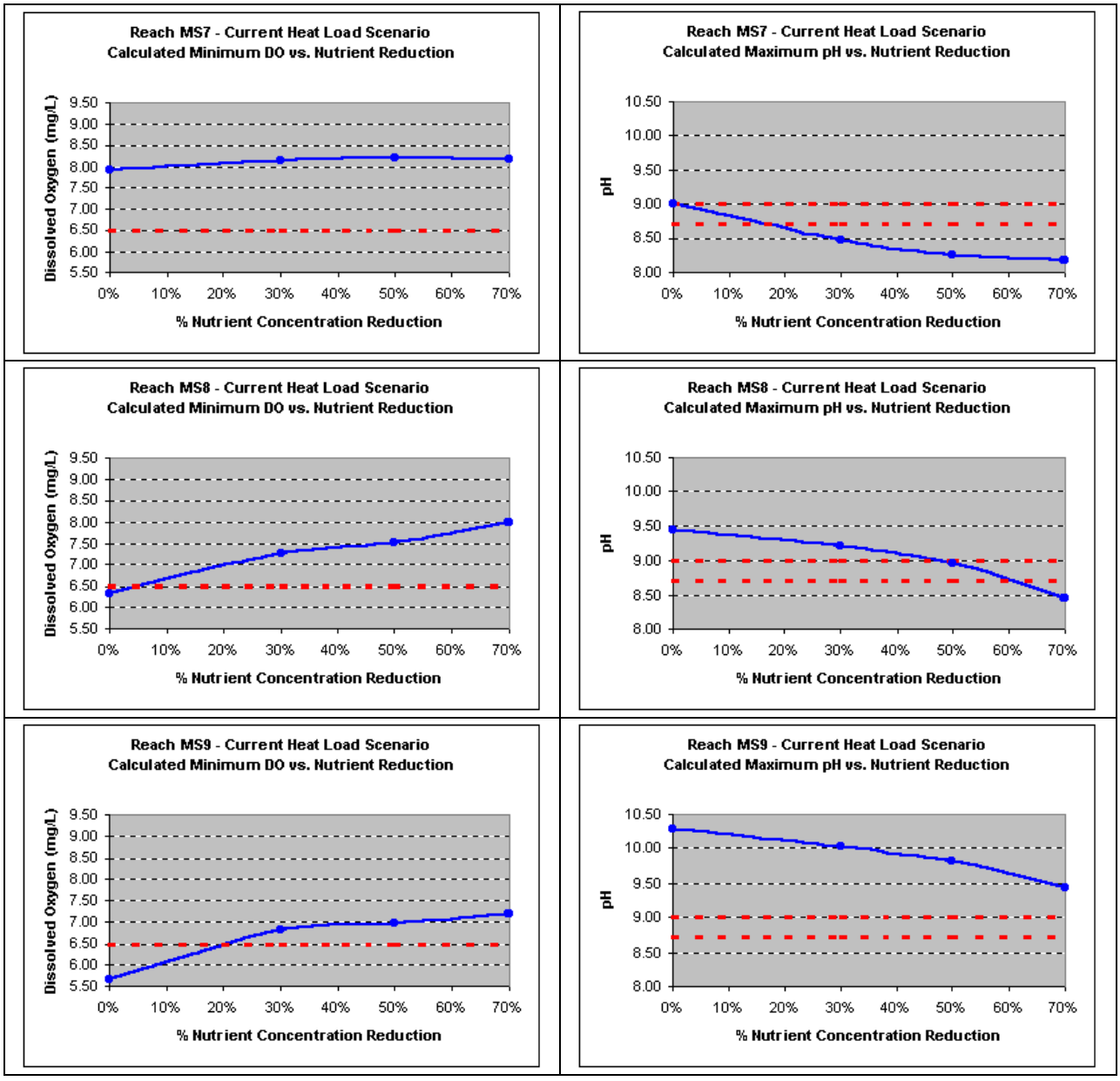

Figure B- 27. Calculated pH and DO for current riparian conditions for various nutrient reductions

5.2 Current Riparian Condition Nutrient Load Allocations

Shown on Figures B-26 and B-27 are two maximum pH standards: 9.0 and 8.7. 8.7 has been applied as the daily maximum standard to provide a margin of safety. For DO, 6.5 mg/L has been applied as the daily minimum standard, which provides for a margin of safety above the 6.0 mg/L absolute minimum criteria and insures that the minimum 30-day average of 8.0 mg/L will be met. Therefore, acceptable scenarios are those in which DO is above 6.5 mg/L and pH is less than 8.7.

As shown in Figures B-26 and B-27, the 6.5 mg/L DO standard is met in all reaches under existing conditions except for reaches MS 8 and 9 (below MP 160.1). However, the 8.7 pH standard is violated in all reaches under existing conditions. In all reaches acceptable load

allocations are controlled by pH, rather than DO, and the load allocations are determined by the % reduction at which the curve meets the standard. Required non-point source (NPS) nutrient concentration reductions (load allocations) and corresponding water column concentrations (loading capacities) are presented in Table B-15.

Table B- 15. Load Allocations for Current Riparian Conditions

Reaches	Milepoints	Nutrient Load Allocations (% Reductions)	Loading Capacities (Water Column Concentrations as Monthly Medians)	
			Dissolved Inorganic Nitrogen µg/L as N	Dissolved Orthophosphate µg/L as P
MS4	Headwaters–182.0	20%	16	8
MS5	182.0-173.0	50%	15	5
MS6	173.0-166.9	35%	23	7
MS7	166.9-160.1	20%	32	12
MS8	160.1-153.8	60%	26	6
MS9	153.8-State Ditch	60% (60% reduction in NPS loads plus summer point source removal)	26	6
	State Ditch - Mouth	60% (60% reduction in NPS loads plus summer point source removal)	26	6

Table B-15 presents nutrient load allocations and loading capacities for both nitrogen and phosphorus. However, only the nitrogen loading capacities directly impact the pH and dissolved oxygen concentrations calculated by the model. This is because the system is nitrogen limited (see Section 4.4) and the growth rate limitation due to nutrients in the model is controlled only by the nutrient in lowest supply relative to cellular requirements. However, to derive loading capacity concentrations for phosphorus, the same percent reductions required for nitrogen have been applied to phosphorus. It is important to reduce phosphorus in addition to nitrogen because in high phosphorus, low nitrogen aquatic environments nuisance blue-green algae (cyanobacteria), which can fix nitrogen, may become established. It is likely that the same measures that reduce nitrogen will provide similar reductions in phosphorus.

Note that in some cases the above dissolved orthophosphate loading capacities may be less than natural background levels. However, it is unclear what the natural background concentrations are, since all reaches in the sub-basin likely receive some degree of anthropogenic nutrient loading. However, it appears that natural background concentrations for dissolved orthophosphate are on the order of about 10 µg/L as P. Therefore, dissolved orthophosphate concentrations less than 10 µg/L as P may not be achievable. Due to uncertainty regarding natural background concentrations, the above loading capacities should be treated only as targets, not standards. Compliance should be based on whether existing standards for dissolved oxygen and pH are achieved, rather than on the above targets for dissolved orthophosphate and DIN.

5.3 Potential Natural Community Scenario

A scenario was modeled in which the potential natural vegetative community was established to its full height and density for a 100 ft distance from the stream for the entire system. For this site potential condition the physiographic vegetative community as shown in Figure B-28 was modeled (Crowe and Clausnitzer, 1997; image by B. Kasper and M. Boyd, Oregon DEQ).

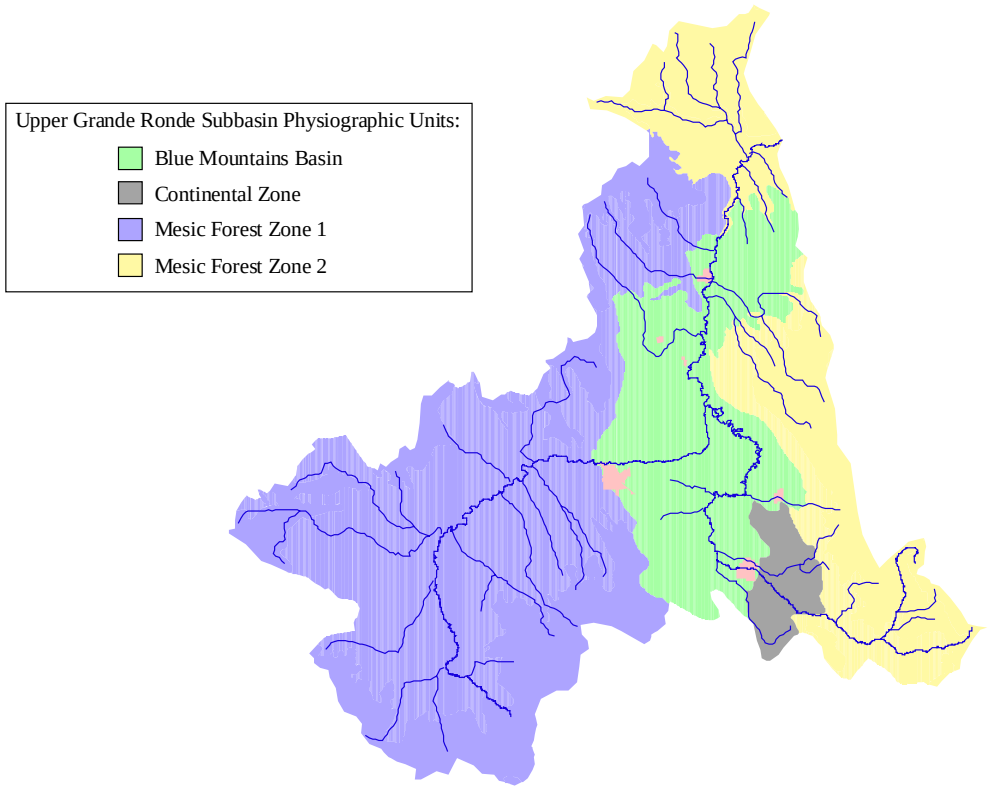

Figure B- 28. Physiographic Units of the Upper Grande Ronde Sub-Basin

Heat Source calculated temperatures and effective shade for this scenario are shown in Table B-16. Calculated pH and DO concentrations for this scenario are presented in Figure B-29 and 30.

Table B- 16. Model inputs for potential natural vegetative community scenarios

Reach	Depth (ft)	Effective Shade (%)	Average Temp (°C)	Max Temp (°C	ΔTemp (°C)
4	0.52	58.5	10.5	13.6	6.2
5	0.72	50.7	11.5	14.1	7.6
6	0.72	50.4	12.3	15.7	6.2
7	0.72	57.3	13.0	14.9	4.0
8	0.81	37.4	14.2	16.4	4.3
9	0.92	60.5	14.6	16.1	3.2

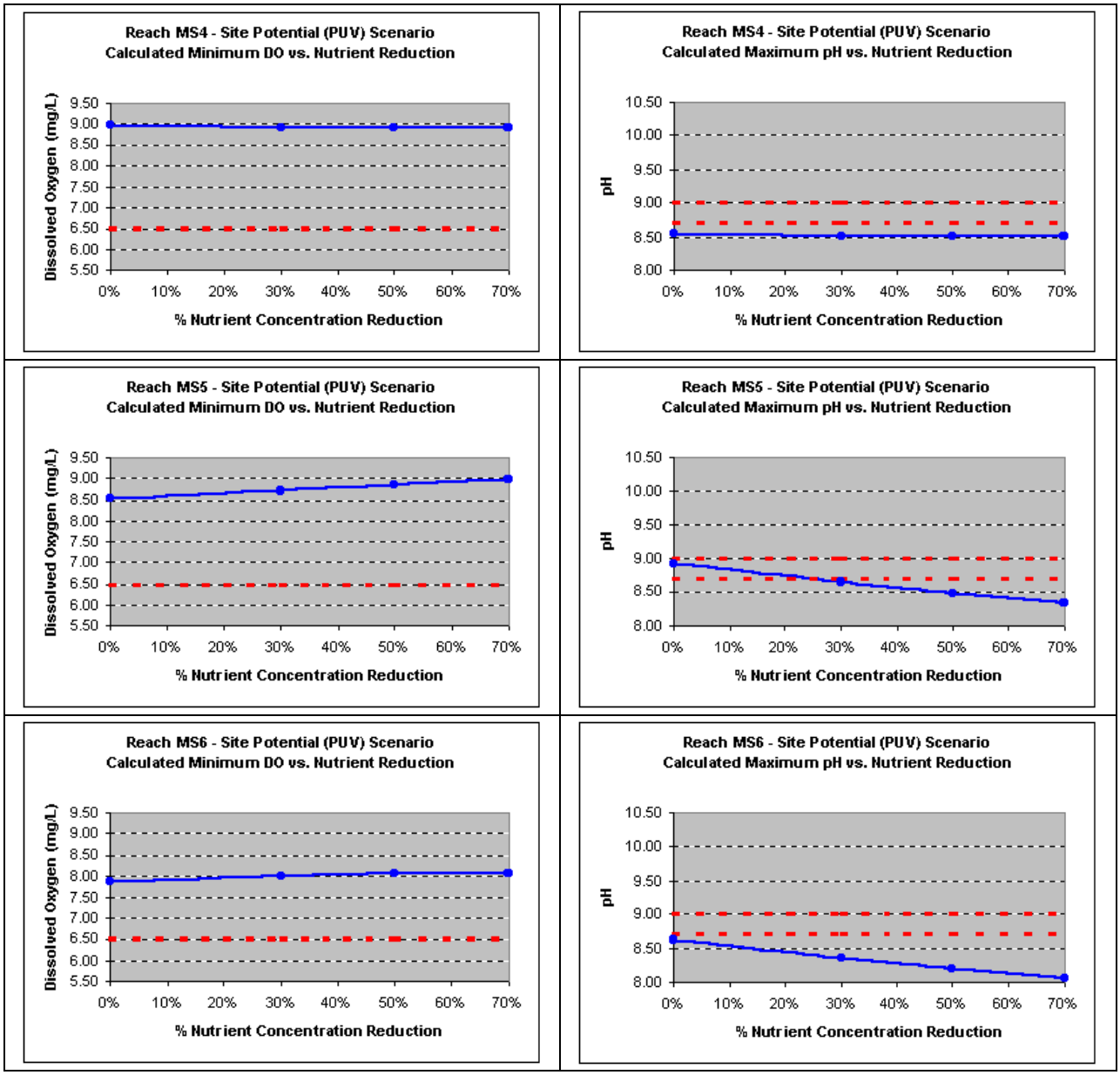

Figure B- 29. Calculated pH and DO for potential natural vegetative community riparian conditions for various nutrient reductions

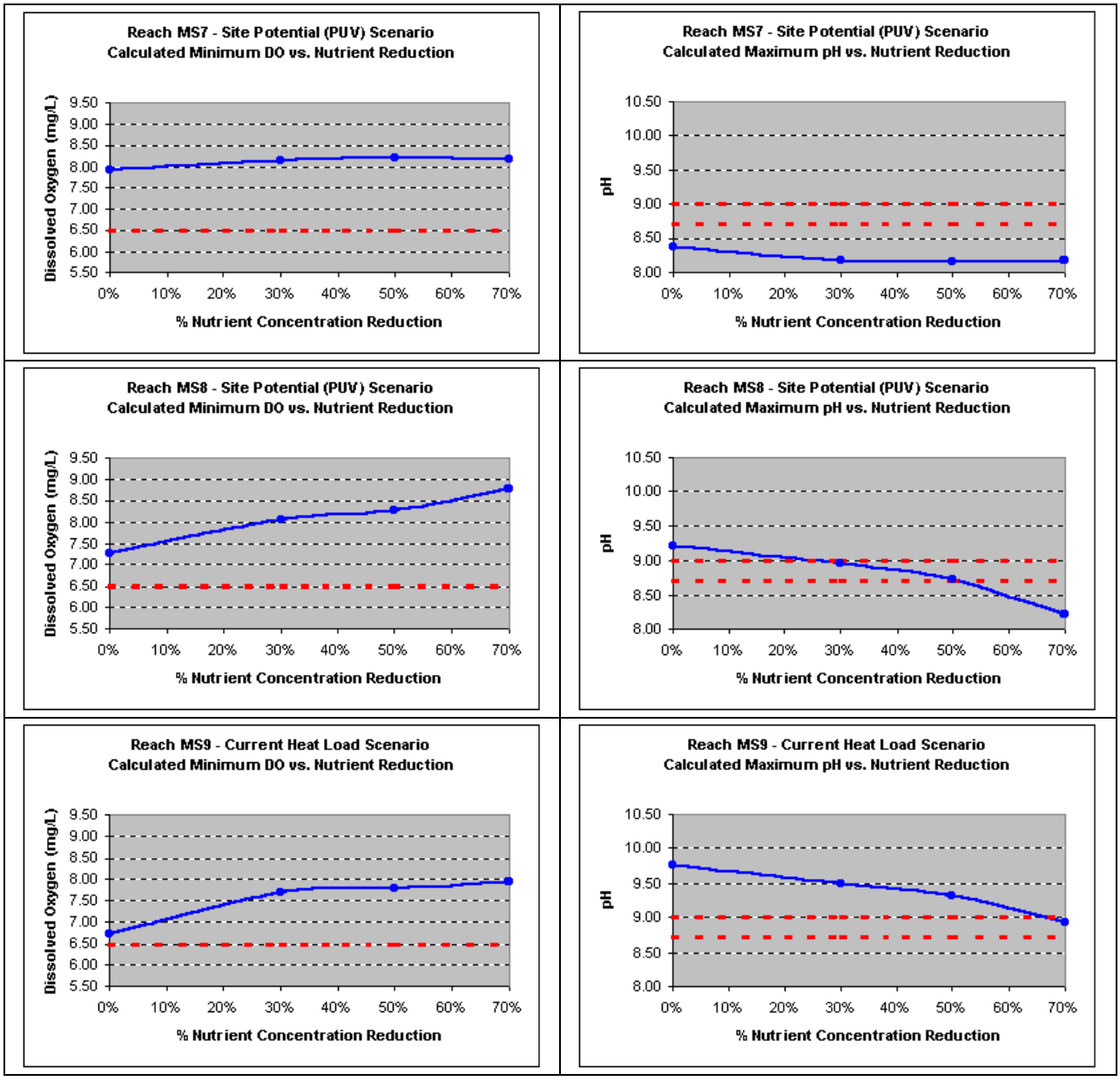

Figure B- 30. Calculated pH and DO for potential natural vegetative community riparian conditions for various nutrient reductions

5.4 Potential Natural Community Scenario Nutrient Load Allocations

As shown in Figures B-29 and B-30, the modeling indicates that if the potential natural community shade scenario is implemented the 6.5 mg/L DO standard will be met in all reaches without additional nutrient reductions. The 8.7 mg/L pH standard would be met in most reaches above MP 160, except for reach MS5 (MP 182.0-173.0), for which a 25% reduction in nutrients would be needed. Below MP 160, significant nutrient reductions would still be needed. Nutrient load allocations for the potential natural community scenario are provided in Table B-17.

Table B- 17. Load Allocations for Potential Natural Vegetative Community Riparian Conditions

Reaches	Milepoints	Nutrient Load Allocations (% Reductions)	Loading Capacities (Water Column Concentrations as Monthly Medians)	
			Dissolved Inorganic Nitrogen µg/L as N	Dissolved Orthophosphate µg/L as P
MS4	Headwaters–182.0	0	20	10
MS5	182.0-173.0	25%	23	7
MS6	173.0-166.9	0%	35	10
MS7	166.9-160.1	0%	40	15
MS8	160.1-153.8	50%	33	7
MS9	153.8-State Ditch	50% (50% reduction in NPS loads plus summer point source removal)	33	7
	State Ditch – Mouth	50% (50% reduction in NPS loads plus summer point source removal)	33	7

As with Table B-15, Table B-17 presents nutrient load allocations and loading capacities for both nitrogen and phosphorus. However, only nitrogen concentrations directly impact the pH and dissolved oxygen concentrations calculated by the model since the system is nitrogen limited. However, to derive loading capacity concentrations for phosphorus, the same percent reductions required for nitrogen have been applied to phosphorus. Due to uncertainty regarding natural background concentrations, the above loading capacities should be treated only as targets. Compliance should be based on whether existing standards for dissolved oxygen and pH are achieved, rather than on the above targets for dissolved orthophosphate and DIN.

5.5 Point Source Wasteload Allocations – City of La Grande WWTP

Upstream of the La Grande Wastewater Treatment Plant, nutrient concentrations in the Grande Ronde River exceed recommended targets for SRP and DIN of 33 and 7 ug/L respectively. These concentrations are significantly increased by the La Grande discharge. Since target concentrations are already exceeded upstream of the discharge, the river has no capacity to assimilate loads from La Grande and the discharge exacerbates already excessive pH and DO fluctuations and standards violations.

Several options exist for mitigating the impact of the La Grande discharge on the Grande Ronde. One option is setting wasteload allocations equal to the lowest levels achievable by available municipal wastewater treatment technology. Concentrations achievable using advanced treatment are <1 mg/L (< 1000 µg/L) for SRP and 3-5 mg/L (3000-5000 µg/L) for DIN (Metcalf & Eddy, 1991). Effluent concentrations of 1 mg/L for SRP and 5 mg/L for DIN would result in the following in-stream concentrations (for the dry weather effluent flow of 4.2 cfs, the 7Q10 river flow of 14 cfs, and assumed background river concentrations of 15 µg/L for SRP and 33 µg/L for DIN):

SRP: 242 µg/L
DIN: 1,179 µg/L

Clearly, even with advanced treatment, nutrient concentrations downstream of the discharge would far exceed target concentrations. Even with advanced treatment, nutrient loads due to the La Grande discharge could be 20-45 times greater than background loads.

A second option is to impose limits adequate to insure that the La Grande discharge does not increase nutrient concentrations in the river beyond the target concentrations. Wasteload allocations for this option would be set equal to river target concentrations of < 10 µg/L as P for dissolved orthophosphate and 26-33 µg/L DIN. Since such stringent limits could not be met using available municipal wastewater treatment technology, this is equivalent to a "no discharge" allocation. This is the most conservative option and is the only option that will insure that nutrient concentrations are not increased by the La Grande discharge and will result in an immediate improvement in downstream pH and dissolved oxygen concentrations.

In the Grande Ronde basin, viable options to river discharge exist for effluent disposal. Non-river effluent disposal in this region is very cost-competitive with advanced treatment. Therefore, since the no discharge option is cost-competitive with advanced treatment and since it will result in the greatest improvement in water quality, no discharge during the critical summer time period is the recommended alternative being pursued by the city.

This no discharge option would remove the effluent during periods of extended low flow when algae are expected to significantly influence water quality. The removal of the point source would not influence the algae growth problems occurring upstream of the discharge nor would it address nutrients which enter the river from non-point source contributions either upstream or downstream of the discharge. The no discharge option would, however, eliminate any further exacerbation of algae growth problems resulting from nutrient contributions of the La Grande waste water treatment plant.

Water quality data was analyzed to determine the critical, no discharge time period (Schnurbusch 1996b, see Appendix). The analysis demonstrates that no discharge should be allowed during the months of July, August, and September. The months of June and October are transitional periods. It has been shown that in June there is a relationship between flow and pH. Standard violations begin to occur in June when the river flow falls below 150 - 200 CFS. Therefore, discharge would need to be discontinued in June when the average daily flow falls below 200 CFS.

During October there is a strong relationship between temperature and pH. Violations of the water quality standard for pH cease when maximum daily stream temperature falls below 15 C. Therefore the wastewater treatment plant would be allowed to resume discharge to the river in October when the maximum daily stream temperature has dropped to the point where it is consistently below 15 C. Alternatively, direct measurement of late afternoon pH could be used as the criteria for resumption of discharge. In October, when the late afternoon pH downstream of the discharge point has reached a level that would provide confidence that no violations of the pH standard would occur, discharge could be resumed. Therefore, it is recommended that discharge not occur in October unless the maximum daily stream temperature is less than 15^0C or the daily maximum pH is less than 8.7.

This "no discharge" option makes the establishment and adoption of WLA for the La Grande treatment plant irrelevant because the plant will contribute no nutrient load to the river during the critical low flow period.

Ammonia toxicity criteria are also exceeded in the Grande Ronde River during the summer months. This is related to the high pH and high water temperature that occurs in the river during these months. Ammonia toxicity will be eliminated following cessation of summer discharge. However, there is still potential for ammonia toxicity during other months of the year. As a result, the permit limitations for the La Grande wastewater treatment plant must include ammonia limitations that will prevent ammonia toxicity and meet DEQ standards for both chronic and acute toxicity (Schnurbusch 1996a, see Appendix).

5.6 Additional Margin of Safety due to Width Reductions

Ignoring the width reductions that will likely occur under the potential natural community scenario has provided additional margin of safety to insure that standards will be met. Restoring the river to site potential conditions will likely result in reduced bank full and wetted widths, increased depths, increased shade, and reduced temperatures. These improvements will reduce diel pH and DO fluctuations beyond that predicted by PCM for the scenario and will provide additional margin of safety that standards will be met.

5.7 Spawning and Egg Incubation Periods

The above allocations were designed to allow pH and DO standards to be met during critical summertime conditions. During fall, winter and spring (October 1 through June 30), the most stringent beneficial use is salmonid spawning and egg incubation, and the applicable water column standard is 95% of saturation. For a 3000 ft. elevation, which is roughly the average elevation of the reaches modeled, 95% saturation at 10^{o}C is 9.7 mg/L, at 12.8^{o}C is 9.1 mg/L, and at 17.8^{o}C is 8.1 mg/L (10^{o}C, 12.8^{o}C and 17.8^{o}C are the temperature standards for Bull Trout, salmonid spawning, and salmonid rearing, respectively).

The non-point source control measures needed to meet the above allocations will apply year round and should result in the 95% of saturation standard being met during all spawning and egg incubation periods. This is because the allocations were designed to meet the more stringent pH standard of 8.7. As shown in Figures B-26, B-27, B-29 and B-30, DO is well above the DO standard whenever the pH standard is met. Therefore, the proposed allocation should result in applicable pH and DO standards being met year-round.

In the fall, winter and spring, from the time flows increase and pH and temperature decline in October until flows decline in June, the La Grande WWTP will be permitted to discharge at its current secondary permit limits. During this period flow rates are much higher than in the summer, and solar radiation and temperature much lower. Therefore, periphyton activity is minimal during this period. In addition, dilution is quite high, which results in no significant impacts due to effluent BOD loads. Therefore, standards for pH and DO should be met during this period, even with the La Grande WWTP discharging at current permit limits.

6 Nutrient Sources and Land Use Specific Load Allocations

6.1 Nutrient Sources

Nutrients enter the system from both point and non-point sources, with the non-point nutrient loads being functions of land use. Above Grande Ronde River MP 160, the basin is comprised mostly of forested public lands. In the Grande Ronde valley below MP 160, the basin is comprised mostly of privately owned agricultural and urban lands. While the valley constitutes less than seven percent of the land in the basin, it contains most of the human population (more than 60 percent) and the vast majority of the crop agriculture in the basin. Forestry and grazing land uses predominate above the valley, while agriculture, urban and grazing land uses predominate within the valley. Significant point sources in the sub-basin include the La Grande wastewater treatment plant, which discharges to the Grande Ronde River, and the City of Union WWTP, which discharges to Catherine Creek. The La Grande WWTP serves a population of approximately 12,900, including the cities of La Grande and Island City. It is the only point source in the sub-basin classified as a "major" facility. The City of Elgin has a wastewater treatment plant but it does not discharge during summer low flow months. There are three additional incorporated communities within the valley: Cove (pop. 545), Imbler (pop. 311), and Summerville (pop. 145). None of these discharge wastewater during summer low flow months.

6.2 Land Use Specific Load Allocations

Figure B-31 overlays land use information and modeling segments (image by B. Kasper, ODEQ using U.S. Geological Survey data).

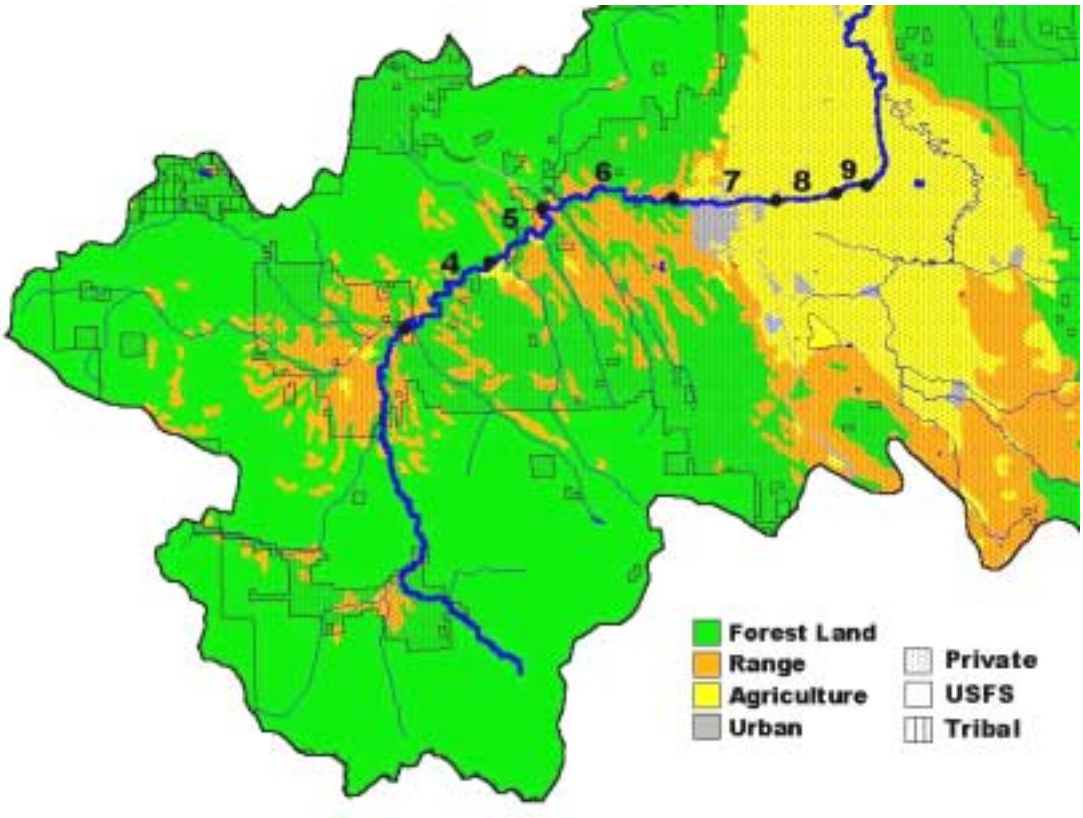

Figure B- 31. Land Use Relative to Modeled Grande Ronde Reaches

As shown, reaches 4, 5 and 6 (MP 166.9 and above) are mixed forest and rangeland. Therefore, all load reductions for these reaches will be allocated to these uses. Reach 7 (MP 166.9-160.1) receives nutrient loads which enter from upstream that are associated with forest and range land uses and loads which enter within the reach that are associated with urban and agricultural land uses. Reach 8 (160.1-153.8) receives non-point source (NPS) loads which enter from upstream that are associated with all of the above and loads which enter within the reach that are primarily associated with agricultural land uses. Reach 9 (153.8-State Ditch) receives non-point source loads from all the above, plus the point source load from the La Grande WWTP.

7 Margin of Safety

Margin of safety has been provided for in the load allocations by:

1) Modeling both dissolved oxygen and pH, rather than taking the traditional approach of simply modeling DO. Since pH was found to control the load allocations, this approach resulted in more stringent load allocations;
2) Applying 8.7 as the absolute maximum pH standard rather than 9.0, and 6.5 mg/L as the absolute minimum DO standard, rather than 6.0 mg/L;
3) Ignoring the benefits of width reductions in potential natural community (site potential) scenarios.

The combined margin of safety provided by the above will ensure that the load allocations proposed will result in the attainment of water quality standards for both pH and dissolved oxygen.